Studies on New Enzymes Responsible for Peptidoglycan Biosynthesis

(ペプチドグリカンの生合成に関与する新規酵素に関する研究)

Feng Ruoyin

Graduate School of Chemical Sciences and Engineering

Hokkaido University

Abstract

Bacterial cell walls contain D-glutamate (Glu) as a component of peptidoglycans. In general, D-Glu is synthesized from L-Glu by Glu racemase (MurI, EC 5.1.1.3). In some bacteria, D-amino acid aminotransferase (EC 2.6.1.21) supplies D-Glu by transamination from D-alanine (Ala) to α-ketoglutarate. However, in my laboratory, detailed bioinformatic analysis was performed and it was revealed that *Xanthomonas oryzae* has no orthologs of both of the genes in spite of the fact that *X. oryzae* is prototroph for D-Glu. This fact strongly suggested that the bacterium would have an alternative D-Glu biosynthetic pathway. In this study, I explored and analyzed the novel enzymes responsible for D-Glu biosynthesis.

In chapter 2, I performed shotgun-cloning experiments with a D-Glu auxotrophic *Escherichia coli* mutant as host and *X. oryzae* as DNA donor. I obtained two complementary genes, *XOO_1319* and *XOO_1320*, which are annotated as a hypothetical protein and MurD (UDP-MurNAc-L-Ala-D-Glu synthetase), respectively. By in vitro experiment with recombinant enzymes, I revealed that XOO_1320 is an enzyme to ligate L-Glu to UDP-MurNAc-L-Ala for the first example of MurD utilizing L-Glu. XOO_1319 is a novel enzyme catalyzing epimerization of the terminal L-Glu of the product in the presence of ATP and Mg^{2+}. XOO_1319 and XOO_1320 were renamed as MurL and MurD2, respectively.

In chapter 3, to study the isomer recognition mechanism of MurD and MurD2, the structure models of MurD2 were constructed based on *E. coli* MurD ($MurD_{ec}$) structure by docking simulations. Several amino acid residues, which were probably responsible for L-Glu recognition, were then replaced with corresponding amino acid residues in $MurD_{ec}$. Consequently, I obtained a mutated MurD2 enzyme accepting only D-Glu as the substrate by two amino acid substitutions. I also tried to convert the

substrate specificity of $MurD_{ec}$ by the same strategy, but the mutated enzymes still accepted only D-Glu. Next, I used another MurD from *Streptococcus mutans* ($MurD_{sm}$) for random screenings of mutant enzymes accepting L-Glu. Consequently, I obtained a mutated $MurD_{sm}$ that had one amino acid substitution and slightly accepted L-Glu. A mutated $MurD_{ec}$ possessing the corresponding one amino acid substitution also accepted L-Glu.

Chapter 4 is the summary of the study.

TABLE OF CONTENTS

Chapter 1

General introduction

1.1 Alternative biosynthetic pathways of primary metabolites in microorganisms

The primary metabolites consist of the vitamins, amino acids, nucleosides and organic acids, which are essential for growth of microorganisms. The biosynthetic pathways of primary metabolites have been well established with model microorganisms such as *Escherichia coli* and *Saccharomyces cerevisiae*. For a long time, the biosynthetic routes established were believed to be common to all microorganisms.

However, in my laboratory, comparative genomics analysis on the absence or presence of orthologs responsible for known biosynthetic pathways has revealed that some microorganisms have alternative pathways for the biosynthesis of primary metabolites.

For example, a novel menaquinone biosynthetic pathway was reported in 2008. Menaquinone is a lipid-soluble electron carrier and a crucial component in the respiratory chain for many bacteria. In *E. coli*, menaquinone is biosynthesized using the well-studied canonical pathway, which requires eight enzymes designated MenA–H (Figure 1.1a). In contract, Hiratsuka *et al.* revealed an alternative biosynthetic pathway operating in *Streptomyces coelicolor,* which utilizes futalosine as a biosynthetic intermediate (Figure 1.1b) (1). Bioinformatic analysis showed that the latter pathway also operates in human pathogens such as *Helicobacter pylori*, which causes stomach cancer. Because menaquinone is essential for the survival of microorganisms, and most useful intestinal bacteria, such as *Lactobacilli*, employ the canonical pathway, the futalosine pathway is an attractive target for the development of specific anti-*H. pylori* drugs.

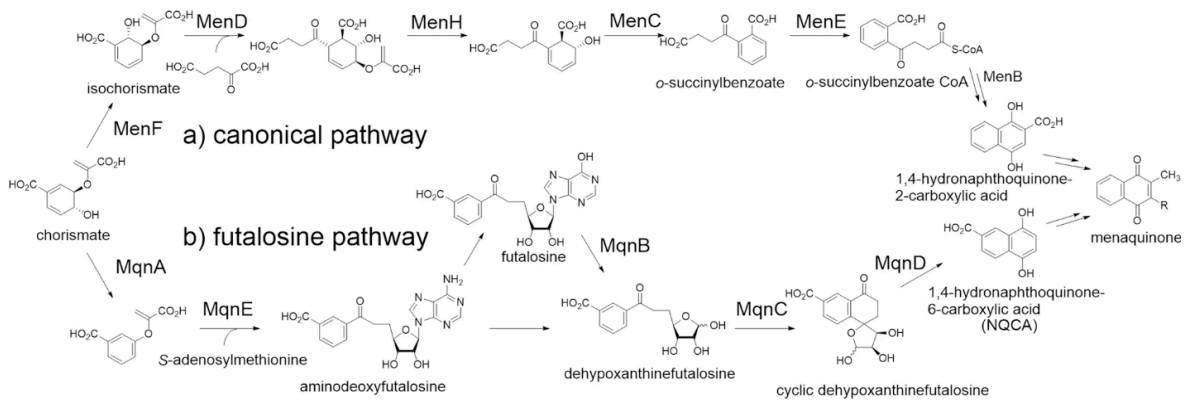

Figure 1.1 Two distinct biosynthetic pathways of menaquinone.
(a) The canonical pathway (b) The futalosine pathway

Similar with menaquinone, folate is necessary for growth of all living cells. *Para*-aminobenzoate, which is a building block of folate, is usually derived from chorismate in the shikimate pathway by reactions of three enzymes designated PabA–C. However, a function unknown enzyme, NE1434, was experimentally confirmed to be responsible for *para*-aminobenzoate biosynthesis in *Nitrosomonas europaea*, which was a prototrophic phenotype to *para*-aminobenzoate despite the fact that there are no orthologs of *pabA*, -*B*, and -*C* in its genome (2). Bioinformatic analysis showed that NE1434 orthologs also operate in obligate intracellular pathogenic bacteria such as *Chlamydia trachomatis* and *Neorickettsia sennetsu.* Since an NE1434 ortholog is absent in most helpful bacteria, NE1434 ortholog would be an attractive target for development of antibiotics with high specificity to human pathogens.

As exemplified by the discovery of these novel biosynthetic pathways (enzymes), microorganisms are expected to have alternative pathways for the biosynthesis of primary metabolites. Since most of the live cells lack these alternative pathways, these pathways would be attractive targets for development of specific antibiotics and pesticides.

1.2 Peptidoglycan biosynthesis

Peptidoglycan is a continuous covalent macromolecular structure found on the outside of the cytoplasmic membrane of almost all eubacteria. Its main function is to preserve cell integrity by withstanding the internal osmotic pressure. Peptidoglycan is also responsible for the maintenance of a defined cell shape, and it is intimately involved in cell growth and cell division. The biosynthetic pathway and mechanism of peptidoglycan have been well studied because the drugs interfering with the proper biosynthesis and assembly of peptidoglycan are effective antimicrobial agents. Indeed, very useful antibiotics such as β-lactams, glycopeptides, and fosfomycin, which inhibit peptidoglycan biosynthesis, have been successfully developed (3–6).

The biosynthesis of peptidoglycan is a complex process that involves about 20 reactions. UDP-*N*-acetylmuramic acid (UDP-MurNAc)-pentapeptide, a unit of peptidoglycan, is synthesized by nine enzymes. Briefly, UDP-*N*-acetylglucosamine (UDP-GlcNAc) is formed from fructose-6-phospate by GlmS, GlmM, and GlmU. Then, UDP-GlcNAc is converted to UDP-MurNAc by MurA and MurB, followed by successive addition of L-Ala, D-Glu, meso-diaminopimelate (or L-Lys), and D-Ala-D-Ala, by four structurally similar enzymes, MurC to MurF (Figure 1.2).

During this process, D-Glu is usually supplied by Glu racemases (MurI) (7). In some microorganisms, D-amino acid aminotransferase supplies D-Glu by transamination from D-Ala to α-ketoglutarate (8). To the best of our knowledge, the D-Glu formation mechanism is limited to these two enzymes in microorganisms.

MurD is the enzyme adding D-Glu to UDP-MurNAc-L-Ala. *E. coli* MurD enzyme has been purified and characterized in the 1990s. The high specificity of *E. coli* MurD for D-Glu was confirmed by studying structurally related analogues tested as substrates or inhibitors. Moreover, L-Glu is absolutely not a substrate of the enzyme (9).

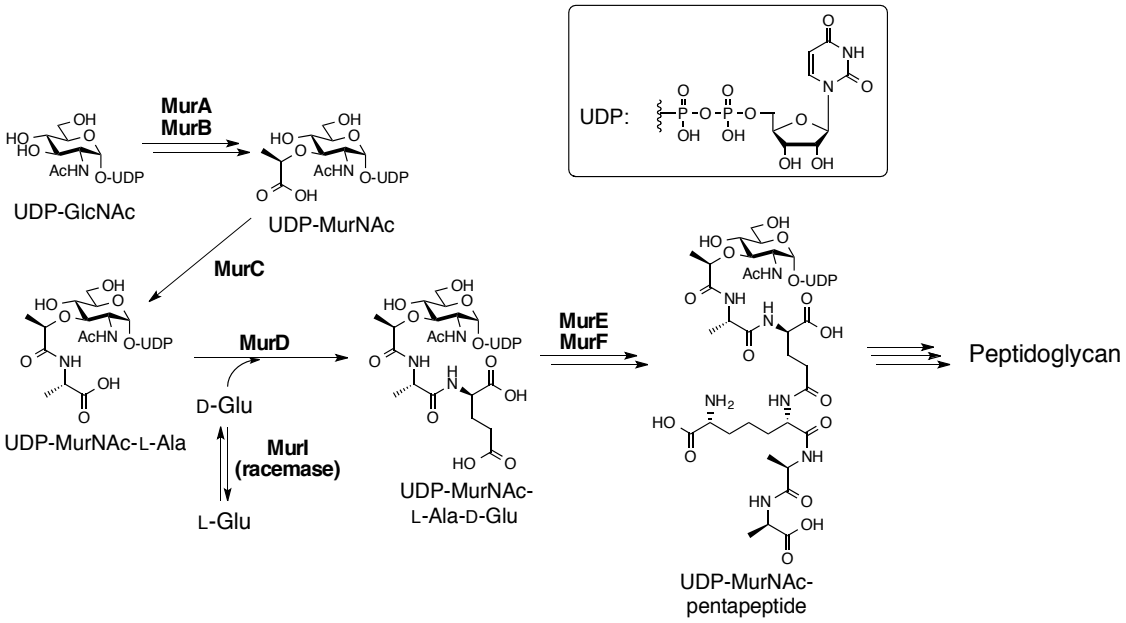

Figure 1.2 Peptidoglycan biosynthetic pathway

Since peptidoglycan is essential for the survival of microorganisms, we examined the presence or absence of orthologs of genes responsible for peptidoglycan formation among bacteria. As a result, it was revealed that *Xanthomonas oryzae* has no orthologs of the Glu racemase or the D-Glu aminotransferase, even though they possess the other Mur orthologs perhaps participating in peptidoglycan biosynthesis, suggesting that *X. oryzae* biosynthesizes D-Glu via an alternative enzyme(s). Since *X. oryzae* causes an important rice disease, the new enzyme(s) would be an attractive target for development of specific pesticides. In this study, I explored and analyzed these new enzymes.

1.3 Peptide epimerization machineries found in microorganisms

D-Amino acid residues have been identified in peptides from microorganisms. Several enzymes, introducing D-amino acid residues into peptides via epimerization, have been reported to date (10).

In bacterial primary metabolisms, enzymes belonging to "enolase superfamily" catalyze the conversion from L-Ala-D-Glu to L-Ala-L-Glu for degradation and recycling of peptidoglycan (Figure 1.3) (11, 12).

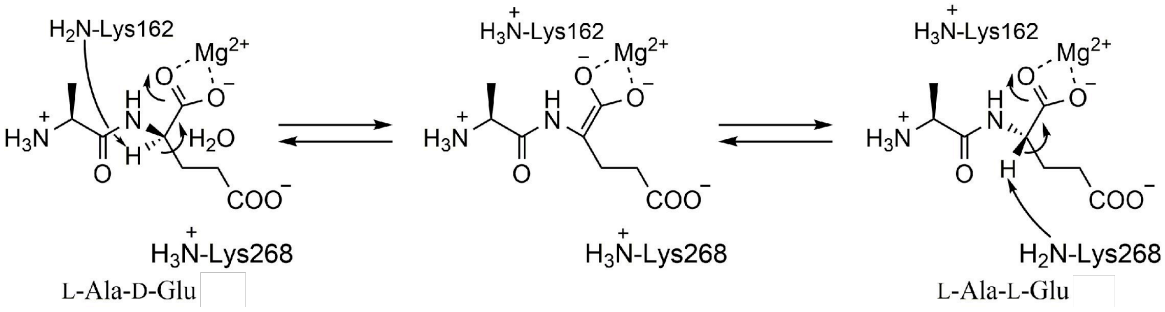

Figure 1.3 Reaction of L-Ala-D/L-Glu epimerases.
A two-base reaction mechanism typical for enolase superfamily enzymes was postulated by X-ray crystallography and mutagenesis studies.

Also, a variety of peptides containing D-amino acid residues have been isolated from microorganisms as secondary metabolites. Their biosynthetic mechanisms have been studied and three different peptide epimerization machineries have been reported.

The first is non-ribosomal peptide synthetase (NRPS). Excellent studies with dissected modules of gramicidin synthetase and tyrocidine synthetase revealed that the epimerization domains embedded in the enzymes catalyze the peptide epimerization (Figure 1.4) (13, 14).

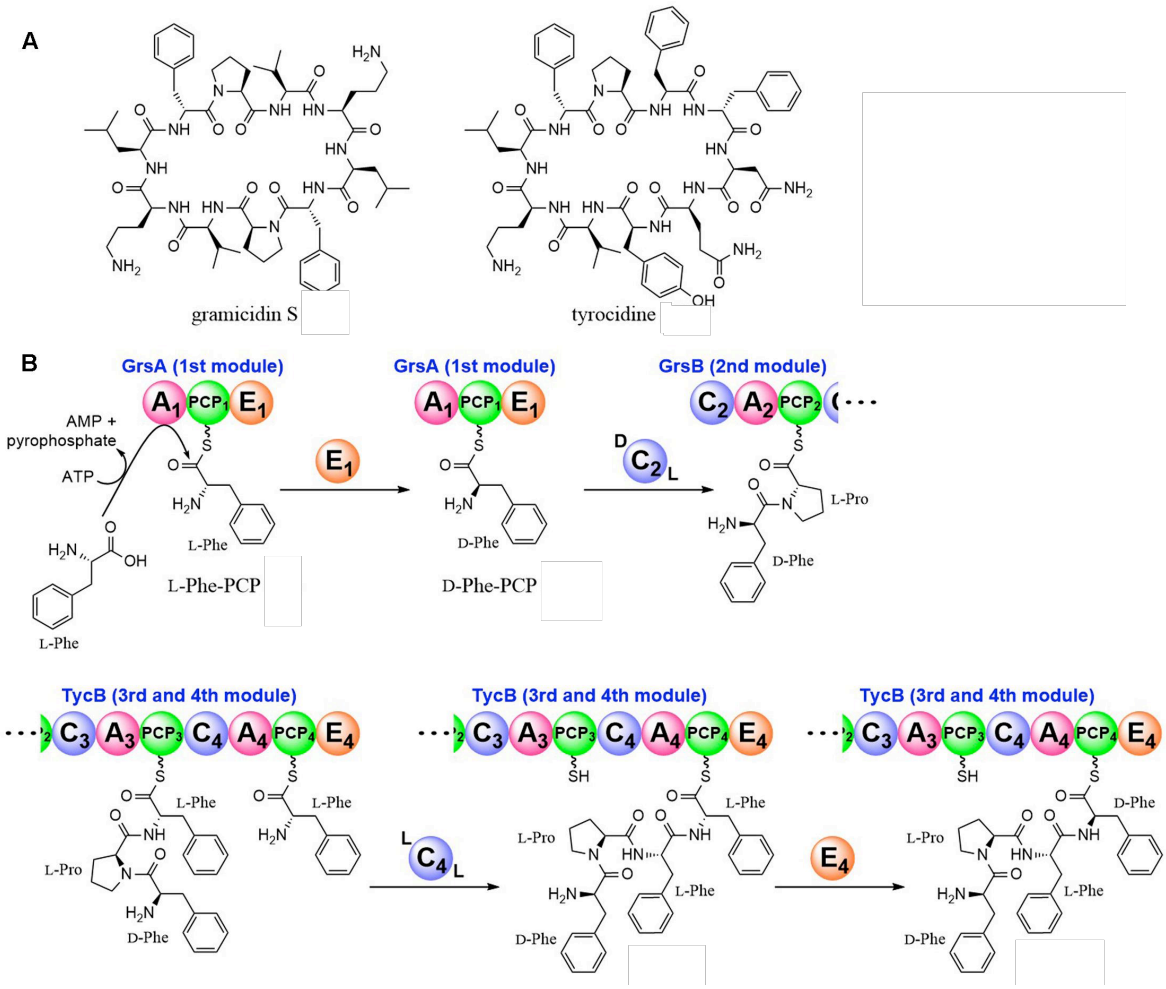

Figure 1.4 Epimerization in NRPS
(A) Structures of gramicidin *S* and tyrocidine. (B) Epimerization reactions by NRPS E domains.

The second type of machinery includes radical-*S*-adenosylmethionine (rSAM)-dependent enzymes, which catalyze a variety of radical-mediated chemical transformations. For example, in the biosynthesis of polytheonamide, a marine sponge-derived and ribosome-dependently supplied peptide composed of 48 amino acids, a rSAM-dependent enzyme is responsible for unidirectional epimerizations of multiple different amino acids in the precursor peptide (Figure 1.5) (15).

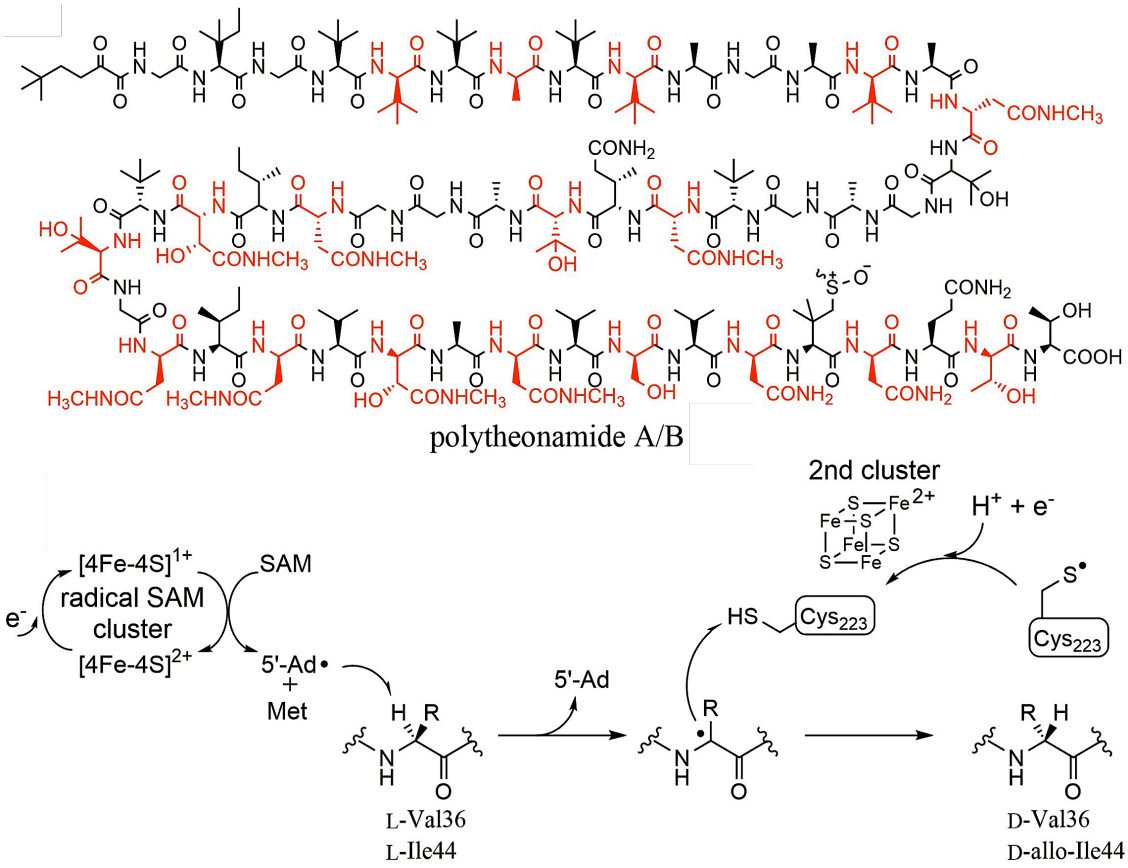

Figure 1.5 Structures of polytheonamide A/B (differing in sulfoxide configuration) and reaction mechanism proposed for rSAM dependent epimerase.
Amino acid residues with D-configuration are shown in red.

The last type of machinery includes the biosynthetic enzymes of lantibiotics, which are ribosome-dependently supplied peptide antibiotics containing polycyclic thioether amino acids (lanthionines). A mechanism for the formation of the D-Ala moiety in lanthionine by two enzymes, dehydratases catalyzing the conversion of L-Ser into dehydroalanine and enzymes catalyzing nucleophilic attack of the thiol of cysteine into dehydroalanine, was clarified (16, 17). Similarly, the formation of a D-Ala residue by reduction of the dehydroalanine residue was also reported (18).

To the best of our knowledge, these machineries are the only examples of peptide epimerization in microorganisms.

However, in this work, I found a novel type of epimerase responsible for D-Glu formation during peptidoglycan biosynthesis. This novel epimerase is the first example utilizing ATP as co-factor.

Chapter 2

Exploration and functional analysis of new enzymes for peptidoglycan biosynthesis

2.1 Introduction

As mentioned in chapter 1, D-Glu is usually supplied by Glu racemases (MurI) (7). In some microorganisms, D-amino acid aminotransferase supplies D-Glu by transamination from D-Ala to α-ketoglutarate (8). To the best of our knowledge, the D-Glu formation mechanism is limited to these two enzymes in microorganisms.

In my laboratory, we have searched for alternative biosynthetic pathways in the primary metabolism to find new targets for development of specific antibiotics and pesticides. Since D-Glu is a necessary component of peptidoglycan, we examined the presence or absence of orthologs of genes responsible for D-Glu formation among bacteria. As a result, it was revealed that *Xanthomonas oryzae*, which causes an important rice disease called bacterial blight (19), has no orthologs of the Glu racemase or the D-Glu aminotransferase (Figure 2.1), even though they possess the other Mur orthologs perhaps participating in peptidoglycan biosynthesis (20), suggesting that *X. oryzae* biosynthesizes D-Glu via an alternative enzyme(s).

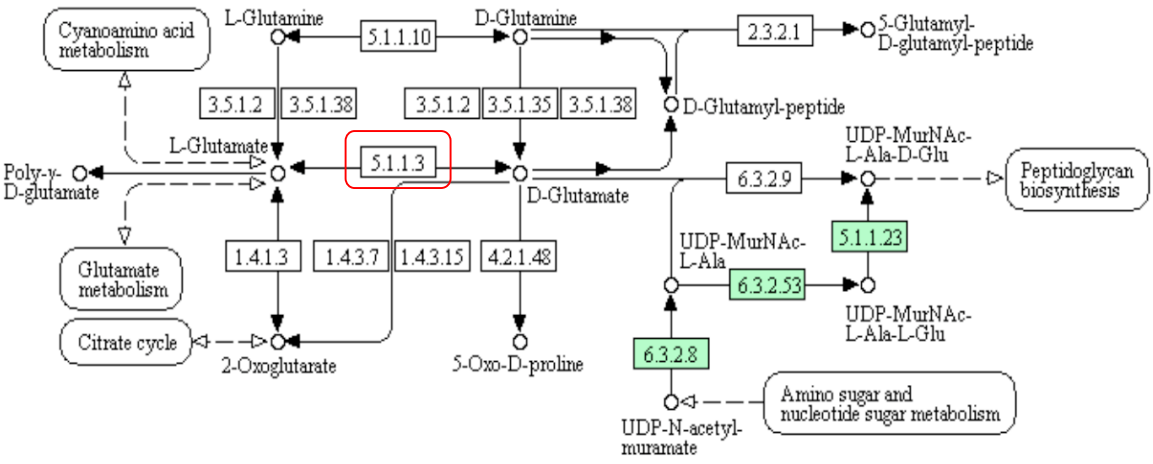

Figure 2.1 D-Glu metabolism in *X. oryzae*.

To discover the gene(s) responsible for D-Glu biosynthesis in *X. oryzae,* I carried out shotgun cloning experiments using a D-Glu auxotrophic *E. coli* mutant WM335 (21) as host and genomic DNA of *X. oryzae* as DNA donor. Consequently, I found two genes, *XOO_1319* and *XOO_1320*, both of which were necessary for complementation of D-Glu auxotroph. To investigate the function of XOO_1319 and XOO_1320, I prepared the recombinant enzymes for in vitro experiments. I confirmed that XOO_1320 was the enzyme to ligate L-Glu to UDP-MurNAc-L-Ala and XOO_1319 was the enzyme catalyzing epimerization of the terminal L-Glu of the product in the presence of ATP and Mg^{2+}. This is the first example for epimerase using ATP as the co-factor.

Moreover, I investigated the occurrence of XOO_1319 and XOO_1320 orthologs among bacteria and found that the orthologs exist in a few strains belonging to Gammaproteobacteria, actinobacteria and Alphaproteobacteria. I found that *Xylella fastidiosa*, which is one of the most dangerous plant bacteria worldwide (22), and *Stenotrophomonas maltophilia*, which is known to cause nosocomial infections (23), also possess the XOO_1319 and XOO_1320 orthologs. Therefore, this alternative peptidoglycan biosynthetic pathway is an attractive target for the development of new antibiotics and pesticides.

In this chapter, the details of these experiments are described.

2.2 Materials and methods

2.2.1 General

UDP-GlcNAc and LB broth (Lennox) medium were purchased from Sigma-Aldrich Japan K.K. (Tokyo, Japan) and L-Ala, L-Glu, and D-Glu were obtained from Wako Pure Chemical Industry (Osaka, Japan). 1-Fluoro-2,4-dinitrophenyl-5-L-alanine amide (L-FDAA) and 1-Fluoro-2,4-dinitrophenyl-5-L-leucine amide (L-FDLA) were purchased from Tokyo Chemical Industry Co. Ltd. (Tokyo, Japan). Other chemicals were analytical grade and purchased from Wako Pure Chemical Industry and Sigma-Aldrich Japan. All restriction enzymes were obtained from Takara Bio (Shiga, Japan), or New England Biolabs Japan (Tokyo, Japan). PCR reactions were carried out using a GeneAmp PCR System 9700 thermal cycler with Tks Gflex DNA polymerase (Takara Bio). Plasmids from *E. coli* were prepared using a Takara Bio plasmid kit. Cell disruption was performed with an ultrasonic disruptor (TOMY, UD-200, Tokyo, Japan). Analysis of the samples during protein purification was performed using sodium dodecyl sulfate (SDS)-polyacrylamide gel electrophoresis (SDS-PAGE), and proteins were visualized by Coomassie brilliant blue staining. Protein concentrations were determined by the Bradford method with bovine serum albumin as a standard.

2.2.2 Bacterial strains and cultures

Xanthomonas oryzae MAFF 311018, *Salinispora tropica* NBRC105044, and *Micromonospora* sp. ATCC 39149 were obtained from The Genetic Resources Center of the National Agriculture and Food Research Organization (Ibaraki, Japan), National Institute of Technology and Evaluation (Tokyo, Japan), and American Type Culture Collection (Manassas, VA, USA), respectively. Genomic DNA of

Stenotrophomonas maltophilia JCM 1975 was provided by the RIKEN BRC through the National Bio-Resource Project of the MEXT, Japan. *Escherichia coli* WM335 was kindly provided by Prof. Dr. Tohru Yoshimura (Nagoya University). LB broth media was used for liquid cultivation. For growth on plates, 1.5% (w/v) agar was added into the media. Ampicillin (Ap), kanamycin (Km), chloramphenicol (Cm), and D-Glu were added to the media at concentrations of 100, 25, 30, and 100 μg mL^{-1}, if necessary.

2.2.3 Shotgun cloning experiment

Genomic DNA of *X. oryzae* MAFF311018 was partially digested with *Sau*3AI and the approximately 5-kbp DNA fragments were separated by agarose gel electrophoresis and then purified. The DNA fragments were ligated into the pUC19 cloning vector (ColE1 ori, P_{lac}, Ap^r; Takara Bio Inc., Shiga, Japan) digested with *Bam*HI. D-Glu auxotrophic *E. coli* WM335 was transformed with the ligation mixture and plated onto LB plates without supplementation of D-Glu.

2.2.4 Subcloning experiment

XOO_1319, *XOO_1320*, and *XOO_1319–1320* were amplified by PCR with appropriate sets of primers (Table 2.1). Each of the amplified fragments was digested with *Nde*I and *Hin*dIII and then inserted into pSTV28N (pSTV28 derivative; pACYC184 ori, P_{lac}, Cm^r) (24) to construct pSTV-XOO_1319, pSTV-XOO_1320, and pSTV-XOO_1319–1320, respectively, for complementation assays.

2.2.5 Preparation of recombinant enzymes XOO_1319, XOO_1320, and MurD

XOO_1319, *XOO_1320*, and *murD* were amplified by PCR using gene-specific primers (Table 2.1). The DNA fragments of *XOO_1319* and *XOO_1320* digested with *Nde*I and *Hin*dIII were inserted into the same sites of the pET28a vector (ColE1 ori, P_{T7}, Km^r; Merck KGaA, Darmstadt, Germany) to construct pET28-XOO_1319 and pET28-XOO_1320. The DNA fragment of *murD* was inserted into the *Bam*HI-*Hin*dIII sites of the pQE80 vector (QIAGEN K.K., Tokyo, Japan) to constructed pQE80-MurD. *Escherichia coli* BL21 (DE3) (Merck) harboring pET28-XOO_1319, pET28-XOO_1320, and pQE80-MurD was separately grown in LB medium (1 L) supplemented with Km or Ap. The strain was grown at 30°C until the OD_{600} reached 2.0 and then isopropyl-β-D-thiogalactopyranoside (0.5 mM) was added to the culture, followed by additional cultivation at 15°C for 16 h. After the cells were harvested and washed once with chilled wash buffer (50 mM sodium phosphate, 300 mM NaCl, 20 mM imidazole, pH 8.0), they were suspended in 40 mL of the wash buffer. Protein purification was carried out using Ni-NTA agarose (QIAGEN). The cells were disrupted by sonication, the debris was removed by centrifugation, and the supernatant was applied to Ni-NTA agarose equilibrated with the wash buffer. The column was washed with the wash buffer and then eluted with elution buffer (50 mM sodium phosphate, 300 mM NaCl, 250 mM imidazole, pH 8.0). All recombinant enzymes were subjected to SDS-PAGE analysis to confirm their molecular sizes and the purified enzymes were used for in vitro assay.

2.2.6 Racemase assay

The standard assay mixture for XOO_1319 contained, in a final volume of 100 μL, 1 mM of L-Glu, 100 mM of Tris-HCl (pH 8.0), and a suitable amount of the

enzyme. Besides this standard assay, additional assays including various co-factors such as PLP and ATP were also performed. The mixture was incubated at 37°C for 16 h. The chirality of the product was analyzed by Marfey's method with L-FDAA (25) as described below.

2.2.7 Preparation of UDP-MurNAc-L-Ala

UDP-MurNAc-L-Ala was enzymatically prepared from UDP-GlcNAc with recombinant His-tagged MurA, MurB, and MurC of *E. coli* using the method described by Raymond *et al* (Figure 1.2) (26). The *murA*, *murB*, and *murC* genes were amplified by PCR with appropriate primers (Table 2.1). Each of the amplified fragments was inserted into the *Bam*HI-*Pst*I sites of the pQE80 vector to construct pQE80-MurA, pQE80-MurB and pQE80-MurC, respectively. After *E. coli* BL21(DE3) was transformed with each of the plasmids, the recombinant enzymes were expressed and purified by the same method as described above.

First, UDP-MurNAc was prepared with recombinant MurA and MurB. The reaction mixture (300 μL) contained 50 mM Tris-HCl (pH 8.0), 15 mM phosphoenol pyruvate, 15 mM β-NADPH, 1 mM dithiothreitol, 5 mM UDP-GlcNAc, and suitable amounts of purified MurA and MurB. The mixture was incubated at 37°C for 16 h and then treated at 95°C for 5 min. After centrifugation, the supernatant was subjected to HPLC. The new product of the reaction was then fractionated and analyzed by high resolution (HR)-ESI-FT-MS (Exactive, Thermo Fisher Scientific Inc., Waltham, MA, USA). The HPLC conditions were as follows: Shimadzu Prominence system (Kyoto, Japan); Mightysil RP-18GP Aqua column (250 mm L × 4.6 mm ID, 5 μm, KANTO CHEMICAL Co., Inc., Tokyo, Japan); flow rate, 1 mL min^{-1}; temperature, 30°C; mobile phase, 50 mM ammonium formate (pH 3.5); detection, 260 nm; injection

volume, 50 μL.

For preparation of UDP-MurNAc-L-Ala, UDP-MurNAc (1 mM) was incubated with a suitable amount of purified MurC in the presence of 100 mM Tris-HCl (pH 8.0), 2.5 mM 2-mercaptoethanol, 20 mM $MgCl_2$, 10 mM ATP, 25 mM $(NH_4)_2SO_4$, and 5 mM L-Ala at 37°C for 16 h. After heat treatment and centrifugation, the supernatant was subjected to HPLC analysis. The new product of the reaction was then fractionated and analyzed by HR-ESI-FT-MS. HPLC conditions were as follows: Shimadzu Prominence system; Develosil RPAQUEOUS column (250 mm L × 4.6 mm ID, 5 μm, Nomura Chemical Co., Ltd., Aichi, Japan); flow rate, 1 mL min^{-1}; temperature, 30°C; mobile phase A, 50 mM ammonium formate (pH 3.5), mobile phase B, methanol; gradient conditions, 2% B, 0–5 min; 2%–50% B, 5–50 min; detection, 260 nm; injection volume, 50 μL.

2.2.8 In vitro assay conditions for recombinant XOO_1320 and MurD

A reaction mixture (100 μL) containing 100 mM Tris-HCl buffer (pH 8.0), 1 mM UDP-MurNAc-L-Ala, 10 mM ATP, 20 mM $MgCl_2$, 2.5 mM 2-mercaptoethanol, 25 mM $(NH_4)_2SO_4$, 5 mM of D-Glu or L-Glu, and various concentrations of the purified recombinant XOO_1320 (50 μg mL^{-1} (0.96 μM), 17 μg mL^{-1} (0.32 μM), and 5.6 μg mL^{-1} (0.11 μM) at final concentrations) was incubated at 37°C for 5 min or 2 h. After heat treatment and centrifugation, the supernatant was subjected to LC-ESI-MS analysis. In addition, both XOO_1320 and XOO_1319 (20 μg mL^{-1} of each enzyme) or MurD (20 μg mL^{-1}) were also used. LC-ESI-MS conditions were as follows: Waters ACQUITY UPLC system equipped with a SQ Detector2 (Tokyo, Japan); Develosil RPAQUEOUS column (150 mm L × 2.0 mm ID, 3 μm, Nomura Chemical Co., Ltd., Aichi, Japan); flow rate, 0.2 mL min^{-1}; temperature, 30°C; mobile phase A,

50 mM ammonium formate (pH 3.5), mobile phase B, methanol; gradient conditions, 2% B, 0–2 min; 2−30% B, 2–30 min; detection, 260 nm; injection volume, 5 μL.

2.2.9 In vitro epimerase assay conditions for recombinant XOO_1319

For the XOO_1319 enzyme assay, enzymatically synthesized and purified UDP-MurNAc-L-Ala-L-Glu was incubated with recombinant XOO_1319 at 37°C for 5 min. The reaction mixture (100 μL) contained 100 mM Tris-HCl buffer (pH 8.0), 1 mM UDP-MurNAc-L-Ala-L-Glu, 10 mM ATP, 20 mM $MgCl_2$, and 20 μg mL^{-1} (0.39 μM) of purified recombinant XOO_1319. LC-ESI-MS conditions were the same as described above. To confirm the reverse reaction, UDP-MurNAc-L-Ala-L-Glu was substituted by UDP-MurNAc-L-Ala-D-Glu that was synthesized enzymatically and purified.

2.2.10 Chiral analysis

The chirality of the product was analyzed using Marfey's method with L-FDAA (25) or L-FDLA (27). First, the product was hydrolyzed at 100°C for 15 h with 3 M HCl. This solution was then evaporated to dryness, and the residues were dissolved in 25 μL of water. To determine the chirality of the assay samples, aliquots (25 μL) of the reaction mixtures were used. To the solution was added 10 μL of 1 M sodium bicarbonate and 50 μL of 1% L-FDAA or L-FDLA dissolved in acetone. The solution was vortexed and incubated at 37°C for 60 min. After the reaction was quenched by the addition of 10 μL of 1 N HCl, the reaction mixture was diluted with 400 μL of methanol. After centrifugation, the supernatant containing L-FDAA derivatives was analyzed by LC-ESI-MS under the following conditions: Waters ACQUITY UPLC system equipped with a SQ Detector2; InertSustain C18 column (150 mm L × 2.1 mm

ID, 3 μm, GL Science Inc., Tokyo, Japan); flow rate, 0.2 mL min^{-1}; temperature, 40°C; mobile phase A, H_2O containing 0.05 vol% trifluoroacetic acid, mobile phase B, methanol containing 0.05 vol% trifluoroacetic acid; gradient conditions, 25% B, 0–2 min; 25–80% B, 2–30 min; detection, 340 nm; injection volume, 5 μL. To detect L-FDLA derivatives, the gradient conditions were as follows; 40% B, 0–2 min; 40%–80% B, 2−30 min.

2.2.11 Preparation of recombinant enzymes of XOO_1319 and 1320 orthologs

XOO_1319 orthologs (*DP16_1118* of *S. maltophilia*, *Strop_3006* of *S. tropica*, and *MCAG_01010* of *Micromonospora* sp.) and *XOO_1320* orthologs (*DP16_1119* of *S. maltophilia*, *Strop_3005* of *S. tropica*, and *MCAG_01009* of *Micromonospora* sp.) were amplified by PCR using gene-specific primers (Table 2.1). The DNA fragments digested with *Nde*I/*Bam*HI or *Nde*I/*Eco*RI were inserted into the same sites of the pET28a vector to express *N*-terminus His-tagged proteins. After *E. coli* BL21(DE3) was transformed with each of the plasmids, the recombinant enzymes were expressed and purified by the same method as described above.

Table 2.1 Primers used for genes expression

Primers	Sequences (5' to 3')
For *XOO_1320* expression	
	ATAGAATTCTTAAGAAGGAGATATACATATGCGAATTTCGCAGTTTGAAGGCAAG
	AGTAAGCTTAATGCACACCCAACCCGGGAATCG
For *XOO_1319* expression	
	ATAGAATTCTTAAGAAGGAGATATACATATGAGCGCTTTCGACAAACATCAGATT
	TATAAGCTTCTAGCCTTCAAACTGCGAAATTCGCACGCAC
For *E. coli murA* expression	
	ATATAGATCTGATAAATTTCGTGTTCAGGGGCAACGAAGCTC
	ATATCTGCAGTTATTCGCCTTTCACACGCTCAATATTTGCACC
For *E. coli murB* expression	
	AGACAGATCTAACCACTCCTTAAAACCCTGGAACACATTTGGC
	ATATCTGCAGTCATGAAATTGTCTCCACTGCGCTCACTTCAC
For *E. coli murC e*xpression	
	ATCCAGATCTAATACACAACAATTGGCAAAACTGCGTTCCATC
	ATATCTGCAGTCAGTCATGTTGTTCTTCCTCCGGAGTTTGC
For *E. coli murD* expression	
	TATGGATCCGCTGATTATCAGGGTAAAAATGTCGTCATTATCGG
	TATAAGCTTCAACCTAACTCCTTCGCCAGACGGGCAAAC
For *DP16_1118* expression	
	GAGATAAACATATGACTGCTTTCGACAAACACCAGGTTTCC
	TATGGATCCTCAAGCTTCGAAATCTTCACGCACCCGTTC
For *DP16_1119* expression	
	GAGATAAACATATGAAGATTTCGAAGCTTGACGGAAAGCGCGTTG
	AAGGGATCCGACCCCTCAGGCGATGC
For *Strop_3005* expression	
	GAGATAAACATATGCGCCTGTCTGACCTGCGCGGACGCAAAG
	AAAGAATTCAGCCGGCGGTGTCGCGGACC
For *Strop_3006* expression	
	GAGATATACATATGCCCAACGAGCAGCTGCGGCGGATG
	TAGAATTCACCCGGGCAGGTTCCGAGCCGGCTCGGTGAG
For *MCAG_01009* expression	

GAGATAAACATATGCGCCTGTCTGACCTGCGCGGACGTACC
AAAGAATTCTAGCGGGCGGGGTGGCCGGCGGTGTC

For *MCAG_01010* expression
GAGATATACATATGCCCAACGAGCAGCTCCGGCGGATG
TATGAATTCACTGCGCGAGGGCCTTGGCGTAGG

Underlining indicates restriction enzyme sites.

2.3 Results

2.3.1 Identification of genes responsible for D-Glu biosynthesis in *X. oryzae*

To search for the gene(s) responsible for the D-Glu biosynthesis in *X. oryzae,* I carried out a shotgun-cloning experiment with D-Glu auxotrophic *E. coli* mutant WM335 as host and genomic DNA of *X. oryzae* as DNA donor. Consequently, I obtained dozens of colonies on LB plates without D-Glu. The transformants were randomly selected and sequences of the inserted DNA were determined. All the inserts had a common region containing 4 genes, *XOO_1318* to *XOO_1321* (20) (Figure 2.2).

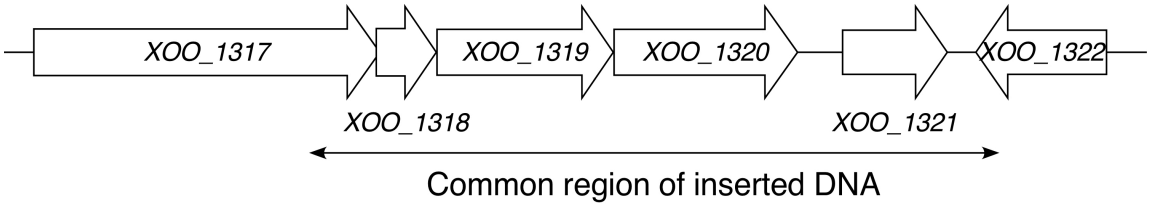

XOO_1318: hypothetical protein
XOO_1319: hypothetical protein
XOO_1320: UDP-MurNAc-L-Ala-D-Glu synthetase (MurD)
XOO_1321: hypothetical protein

Figure 2.2 DNA regions complementing the D-Glu auxotrophic *E. coli* mutant.

To determine the essential gene(s) for the complementation of D-Glu-auxotroph, the inserted DNA fragment was subcloned and used again for the complementation assay. Finally, it was revealed that two genes, *XOO_1319* and *XOO_1320*, which are annotated as a function unknown protein and MurD, respectively, were essential and neither XOO_1319 nor XOO_1320 complemented the D-Glu auxotrophy (Figure 2.3).

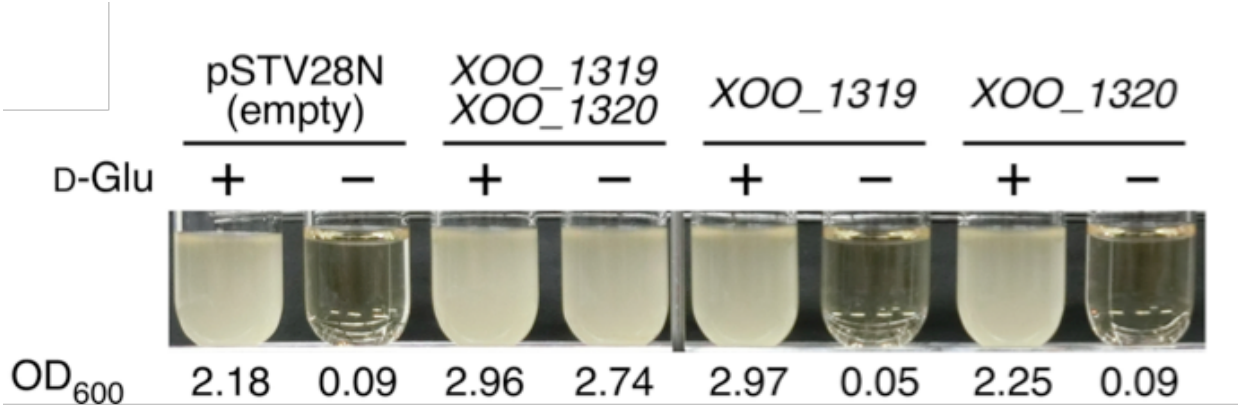

Figure 2.3 Complementation assay of the D-Glu auxotrophic *E. coli* mutant with subcloned plasmids.

2.3.2 Function analysis of XOO_1319 and XOO_1320

2.3.2.1 Preparation of recombinant enzymes of XOO_1319, XOO_1320, and MurD

To study the detailed mechanism of D-Glu formation, recombinant enzymes of XOO_1319 and XOO_1320 were prepared for in vitro experiments. Since XOO_1320 has a 26% identity with MurD from *E. coli*, MurD was also prepared as a comparison. His-tagged recombinant enzymes were successfully expressed in a soluble form. The obtained recombinant XOO_1319, XOO_1320, and MurD, which had a calculated molecular mass of 51.3 kDa, 51.9 kDa, and 48.2 kDa, respectively, were subjected to SDS-PAGE analysis to confirm the molecular size and purity (Figure 2.4).

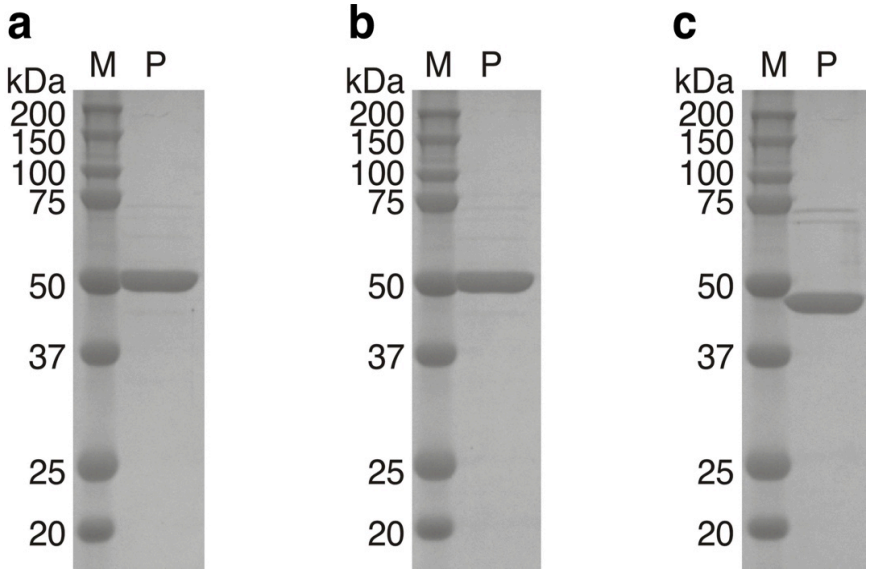

Figure 2.4 Expression and purification of recombinant XOO_1319, XOO_1320, and MurD.
(a) SDS-PAGE analysis of purified XOO_1319 (51.3 kDa). M, marker; P, purified protein. (b) SDS-PAGE analysis of purified XOO_1320 (51.9 kDa). M, marker; P, purified protein. (c) SDS-PAGE analysis of purified MurD (48.2 kDa). M, marker; P, purified protein.

2.3.2.2 Preparation of substrate UDP-MurNAc-L-Ala

UDP-MurNAc-L-Ala was enzymatically prepared from UDP-GlcNAc with recombinant His-tagged MurA, MurB, and MurC of *E. coli* using the method described by Raymond *et al*. (26).

2.3.2.2.1 Preparation of recombinant enzymes of MurA, MurB and MurC

His-tagged recombinant enzymes were successfully expressed in a soluble form. The obtained recombinant MurA, MurB, and MurC, which had a calculated molecular mass of 46.1 kDa, 39.1 kDa, and 54.9 kDa, respectively, were subjected to SDS-PAGE analysis to confirm the molecular size and purity (Figure 2.5).

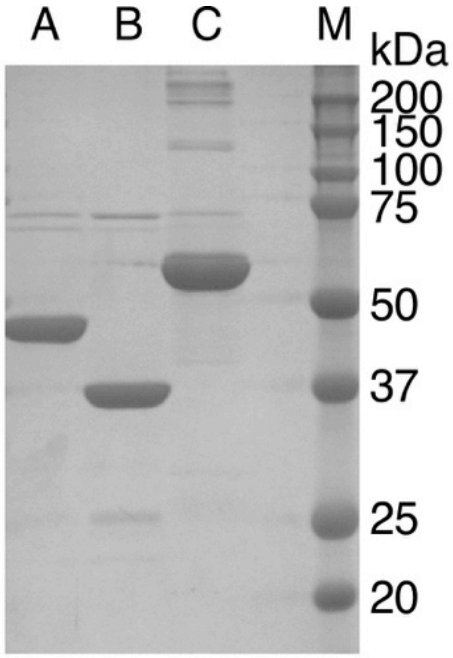

Figure 2.5 Expression and purification of recombinant MurA, MurB, and MurC of *E. coli*.
M, marker; A, purified MurA (46.1 kDa); B, purified MurB (39.1 kDa); C, purified MurC (54.9 kDa).

2.3.2.2.2 Preparation of UDP-MurNAc with recombinant MurA and MurB

For UDP-MurNAc synthesis, UDP-GlcNAc was incubated with purified MurA and MurB. By HPLC analysis, a new product was detected (Figure 2.6 (a)). The product was then fractionated and analyzed by high resolution (HR)-ESI-FT-MS (Exactive, Thermo Fisher Scientific Inc., Waltham, MA, USA). Based on the analysis (m/z: $[M-H]^-$ calculated for $C_{20}H_{30}O_{19}N_3P_2$, 678.09542; observed, 678.09682), the molecular formula of the product was determined to be $C_{20}H_{31}O_{19}N_3P_2$, which corresponded to UDP-MurNAc, confirming the formation of UDP-MurNAc.

2.3.2.2.3 Preparation of UDP-MurNAc-L-Ala using recombinant MurC

For UDP-MurNAc-L-Ala synthesis, UDP-MurNAc and L-Ala was incubated with purified MurC. By HPLC analysis, a new product was detected (Figure 2.6 (b)). The product was then fractionated and analyzed by HR-ESI-FT-MS. Based on the HR-ESI-FT-MS analysis (m/z: $[M-H]^-$ calculated for $C_{23}H_{35}O_{20}N_4P_2$, 749.13254; observed, 749.13449), the molecular formula of the product was determined to be $C_{23}H_{36}O_{20}N_4P_2$, which corresponded to UDP-MurNAc-L-Ala, confirming the formation of UDP-MurNAc-L-Ala.

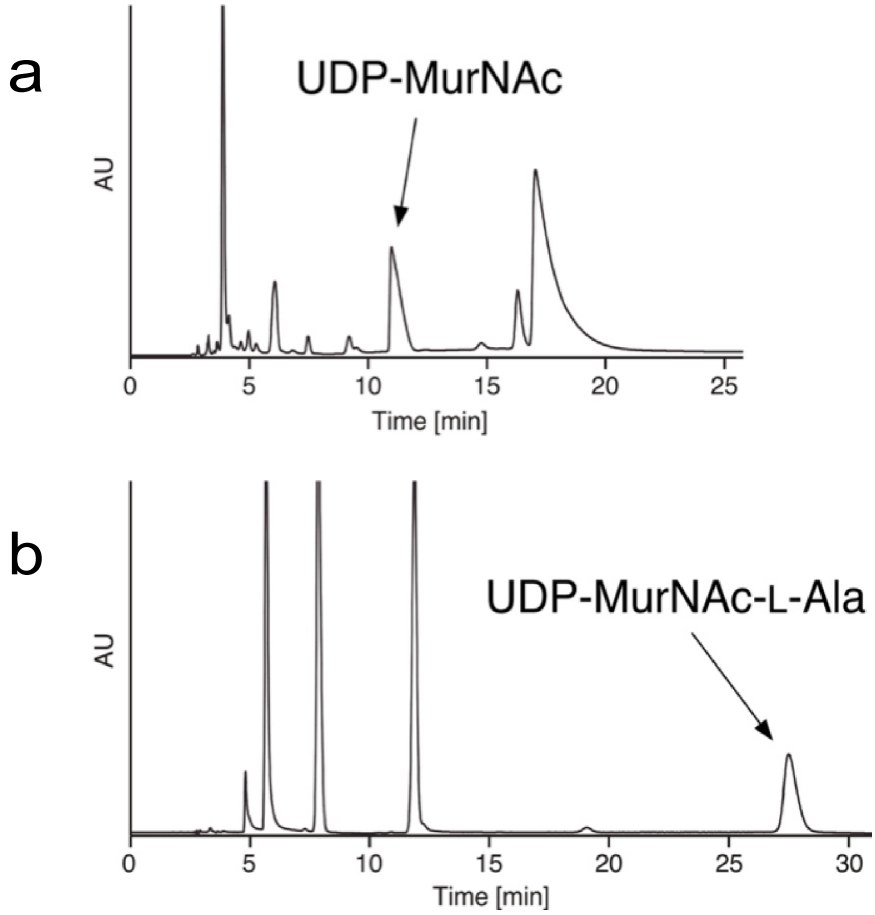

Figure 2.6 Preparation of UDP-MurNAc-L-Ala.

(a) HPLC analysis of enzymatically prepared UDP-MurNAc. Based on HR-ESI-FT-MS analysis (m/z: $[M-H]^-$ calculated for $C_{20}H_{30}O_{19}N_3P_2$, 678.09542; observed, 678.09682), the molecular formula of the product was determined to be $C_{20}H_{31}O_{19}N_3P_2$. (b) HPLC analysis of enzymatically prepared UDP-MurNAc-L-Ala. Based on HR-ESI-FT-MS analysis (m/z: $[M-H]^-$ calculated for $C_{23}H_{35}O_{20}N_4P_2$, 749.13254; observed, 749.13449), the molecular formula of the product was determined to be $C_{23}H_{36}O_{20}N_4P_2$.

2.3.2.3 Racemase assay with XOO_1319 and D-Glu ligase assay with XOO_1320

Since XOO_1320 has similarity to MurD and possibly ligates D-Glu to UDP-MurNAc-L-Ala, XOO_1319 was suggested to be a Glu racemase (Scheme 2.1). To examine this possibility, I carried out the racemase assay using recombinant XOO_1319 and MurD assay (UDP-MurNAc-L-Ala-D-Glu ligase assay) using recombinant XOO_1320.

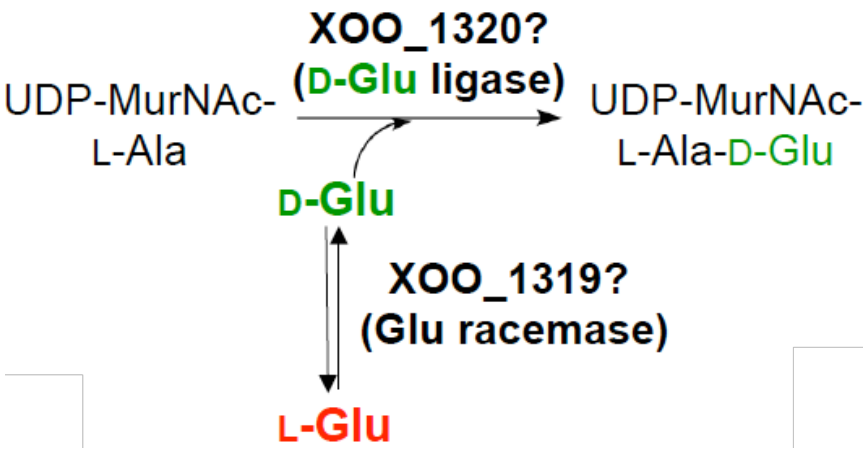

Scheme 2.1 Proposed peptidoglycan biosynthetic pathway by racemase and D-Glu ligase.

2.3.2.3.1 Racemase assay with XOO_1319

To investigate whether XOO_1319 had the predicted Glu racemase activity, I performed in vitro experiments with recombinant XOO_1319 and L-Glu as the substrate under various conditions. Chiral analysis of the products was performed by Marfey's method using L-FDAA (25).

However, the enzyme showed no racemase activity even with reaction mixtures containing pyridoxal-5'-phosphate (PLP), which is an essential co-factor for typical amino acid racemases. The racemase activity was also undetected with both XOO_1319 and XOO_1320 (Figure 2.7).

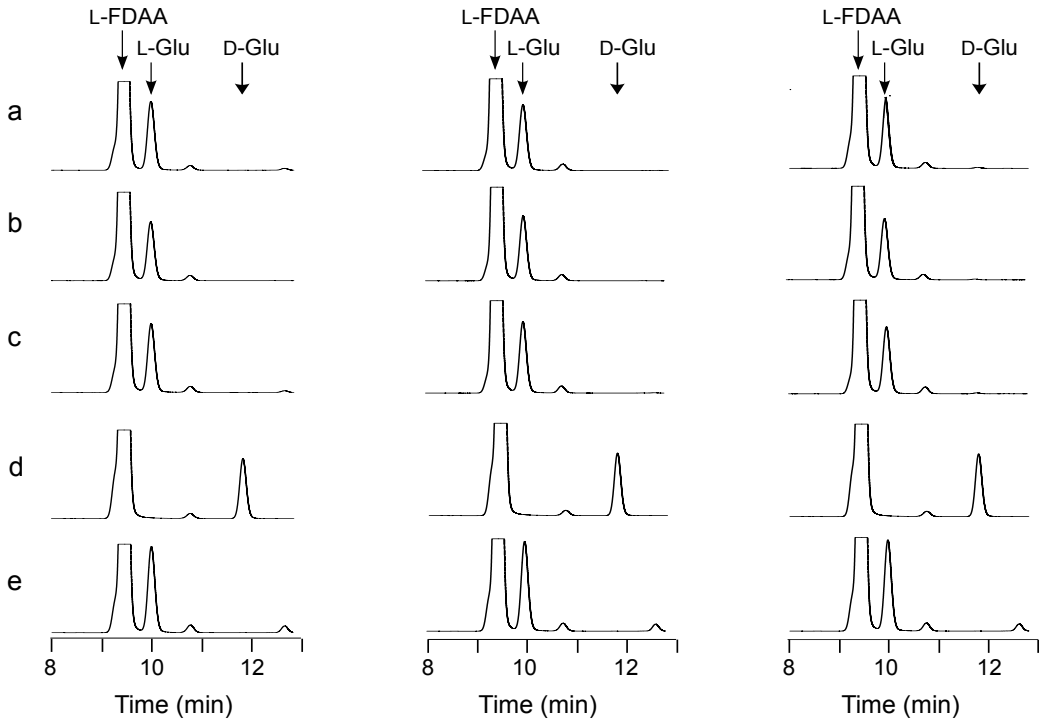

Figure 2.7 Racemase assay with recombinant XOO_1319.
The chirality of Glu was analyzed using L-FDAA. HPLC traces of the reaction products under the standard reaction conditions (left column), including ATP and $MgSO_4$ (middle column), and PLP (right column) are shown. Traces a, b, and c indicate the reactions with XOO_1319, both XOO_1319 and XOO_1320, and no enzyme, respectively. The standards, D-Glu (trace d) and L-Glu (trace e), were also analyzed.

2.3.2.3.2 UDP-MurNAc-L-Ala-D-Glu ligase assay with XOO_1320

To investigate whether XOO_1320 had the predicted UDP-MurNAc-L-Ala-D-Glu ligase activity. Recombinant XOO_1320 was incubated with UDP-MurNAc-L-Ala and D-Glu in the presence of ATP and Mg^{2+}. However, extremely small amounts of the product UDP-MurNAc-L-Ala-D-Glu were detected only when large amounts of recombinant XOO_1320 (50 μg mL^{-1}, 0.96 μM) were used and incubated for 2 h, showing that XOO_1320 had a very weak D-Glu ligase activity (Figure 2.8).

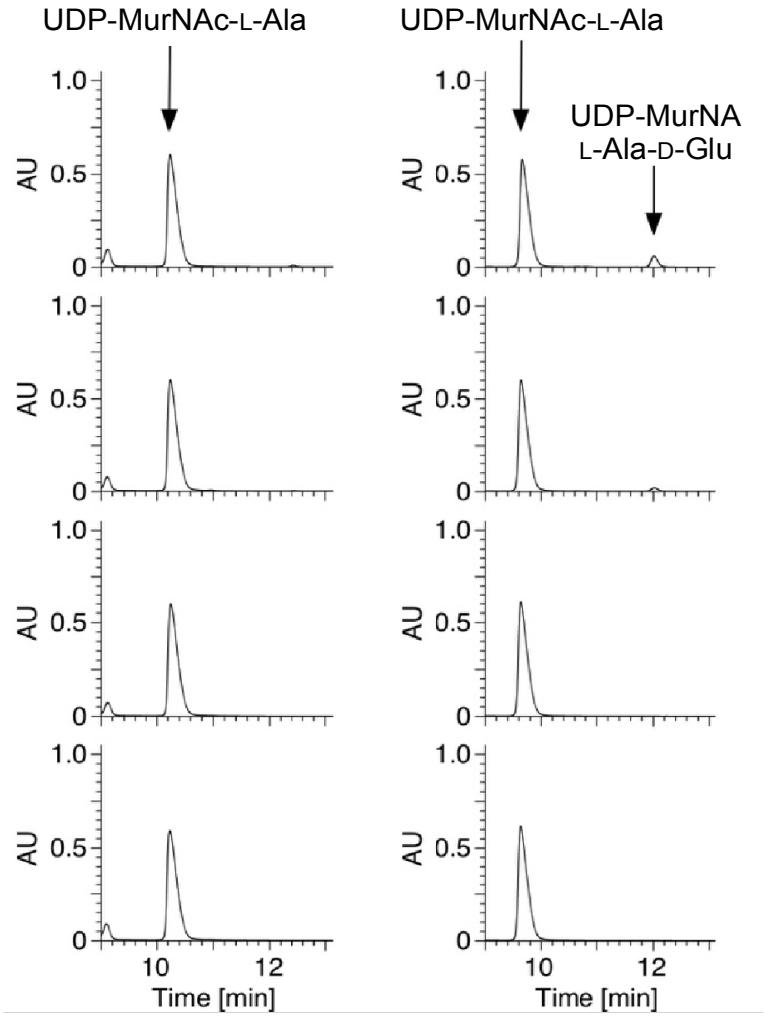

Figure 2.8 Glu ligase assay with recombinant XOO_1320 using D-Glu as substrate. HPLC traces of the reaction products formed with 50, 17, and 5.6 μg mL^{-1} (0.96, 0.32, and 0.11 μM) of XOO_1320 and boiled XOO_1320 (from top to bottom) after 5 min (left column) and 2 h (right column) reaction times are shown.

2.3.2.4 L-Glu ligase assay with XOO_1320 and Glu epimerase assay with XOO_1319

2.3.2.4.1 In vitro assay with both enzymes using L-Glu as substrate

As mentioned above, both XOO_1319 and XOO_1320 were shown to be essential by the genetic complementation experiment. Also, D-Glu is usually supplied from L-Glu. I therefore incubated both recombinant enzymes with UDP-MurNAc-L-Ala and L-Glu under the same reaction conditions.

By LC-MS analysis, I surprisingly and unexpectedly detected large amounts of a new product. This new product had the same elution time as UDP-MurNAc-L-Ala-D-Glu formed by *E. coli* MurD with UDP-MurNAc-L-Ala and D-Glu as the substrates (Figure 2.9). The new product also had the same mass spectrum with UDP-MurNAc-L-Ala-D-Glu (Figure 2.10). In contrast, no products were formed when D-Glu was used as the substrate.

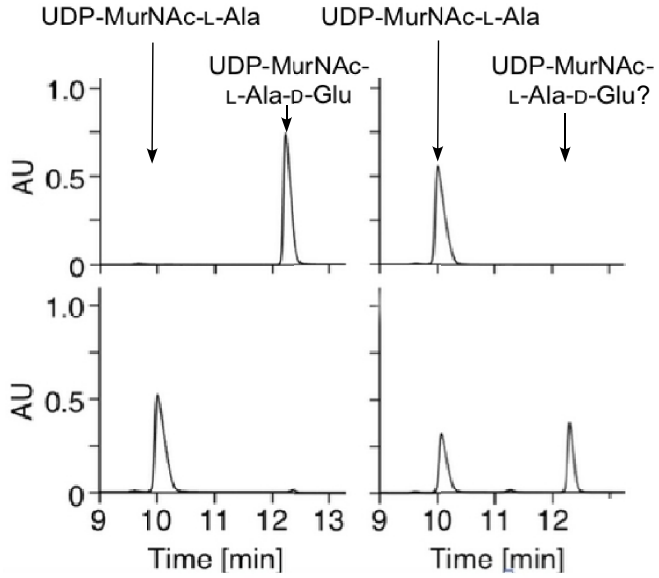

Figure 2.9 UDP-MurNAc-L-Ala-L/D-Glu synthetase activities.
E. coli MurD (top), and a mixture of XOO_1320 and XOO_1319 (bottom) were incubated with UDP-MurNAc-L-Ala and D-Glu (left column) or L-Glu (right column). HPLC traces of the reaction products are shown.

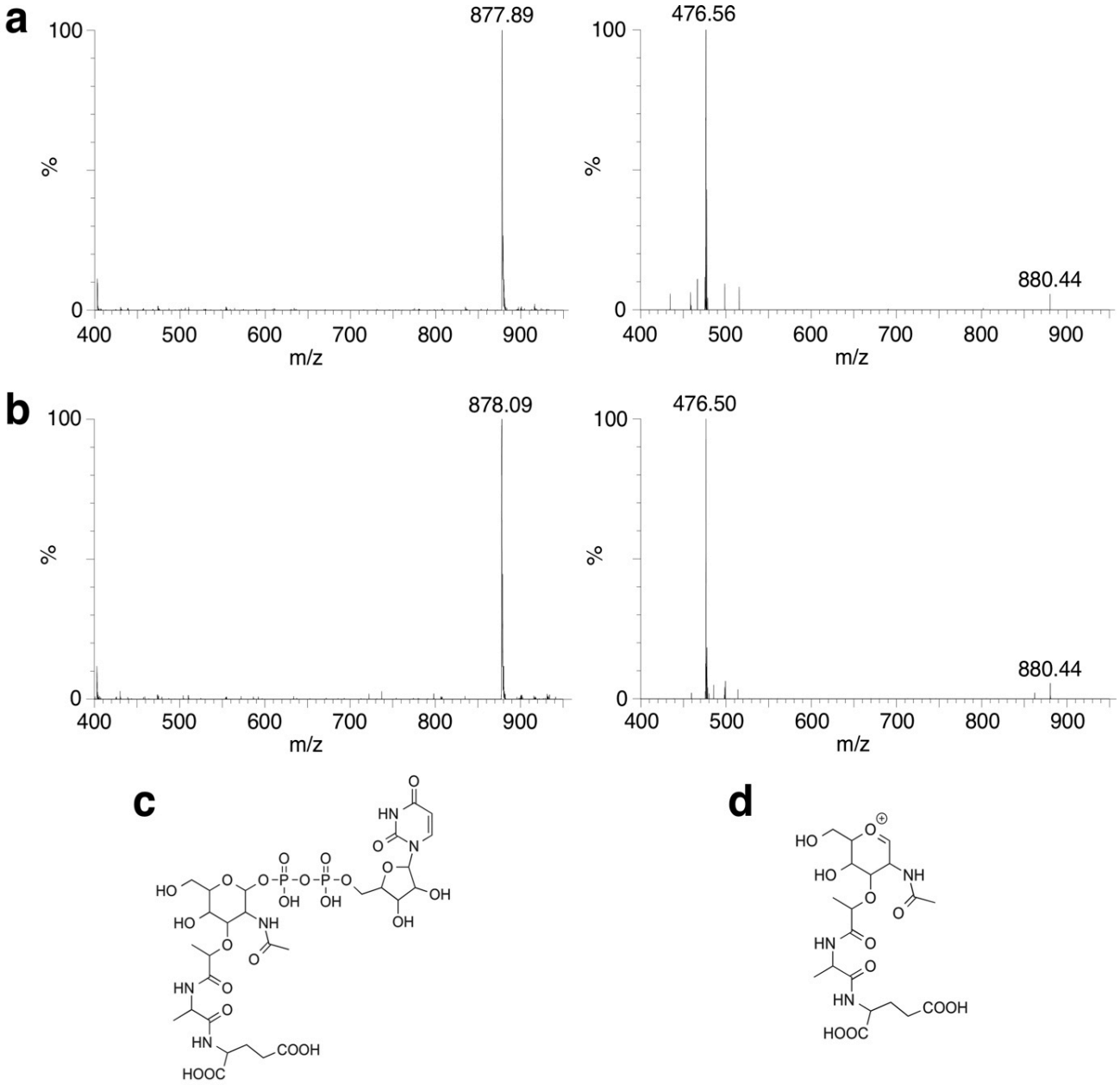

Figure 2.10 Mass spectra of the reaction products of MurD and a mixture of XOO_1319 and XOO_1320.

(a) Mass spectra of the reaction products of MurD (left, ESI negative mode; right, ESI positive mode). Based on HR-ESI-FT-MS analysis (m/z: $[M-H]^-$ calculated for $C_{28}H_{42}O_{23}N_5P_2$, 878.17513; observed, 878.17744), the formation of UDP-MurNAc-L-Ala-D-Glu was confirmed. An oxonium ion derived from UDP-MurNAc-Ala-Glu (calculated molecular mass, 476.18749) was also detected as a major fragment as described Raymond *et al*. (6). (b) Mass spectra of the reaction products of a mixture of XOO_1319 and XOO_1320 (left, ESI negative mode; right, ESI positive mode). An oxonium ion was also detected as a major fragment. (c) Chemical structure of UDP-MurNAc-Ala-Glu (molecular formula, $C_{28}H_{43}O_{23}N_5P_2$; calculated mass, 879.18241). (d) Chemical structure of the oxonium ion derived from UDP-MurNAc-Ala-Glu (calculated mass, 476.18749).

To confirm whether this new product was UDP-MurNAc-L-Ala-D-Glu, I examined the chirality of the terminal Glu moiety of the product by a modified Marfey's method (27). The product purified with HPLC was hydrolyzed under acid conditions, and the released amino acid was reacted with L-FDLA. LC-MS analysis revealed the reaction product contained only D-Glu (Figure 2.11). Consequently, this new product was proved to be UDP-MurNAc-L-Ala-D-Glu.

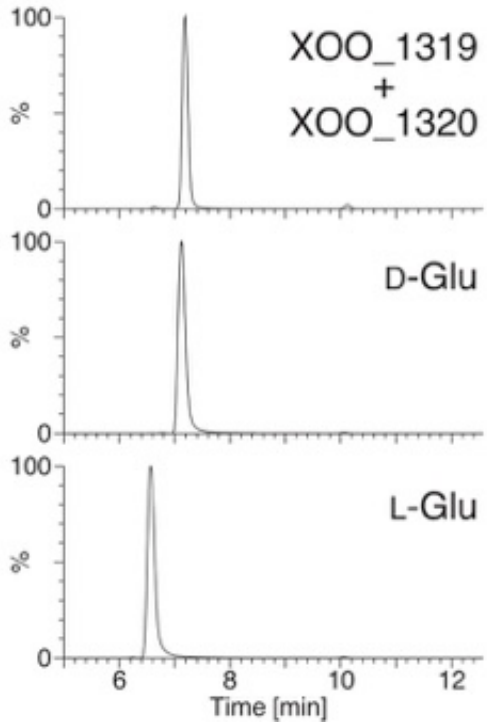

Figure 2.11 Chiral analysis of the terminal Glu residue of the product formed from UDP-MurNAc-L-Ala and L-Glu with recombinant XOO_1319 and XOO_1320.
L-FDLA derivatives of Glu released by acid hydrolysis of the reaction product were analyzed by LC-MS with selected ion monitoring at m/z 440, corresponding to $[M-H]^-$ of the FDLA derivative of Glu. The standards, D-Glu (middle) and L-Glu (lower), were also analyzed.

Based on these observations, I hypothesized that XOO_1320 and XOO_1319 were a UDP-MurNAc-L-Ala-L-Glu synthetase and an L-Glu epimerase of the product (glycopeptidyl-glutamate epimerase), respectively (Scheme 2.2).

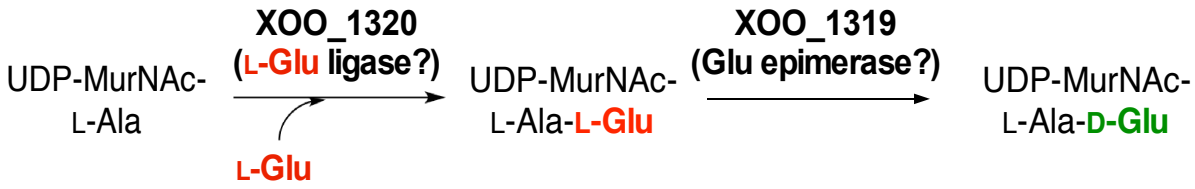

Scheme 2.2 Proposed peptidoglycan biosynthetic pathway by L-Glu ligase and epimerase

To examine this possibility, I performed the UDP-MurNAc-L-Ala-L-Glu ligase assay with recombinant XOO_1320 and Glu epimerase assay with recombinant XOO_1319.

2.3.2.4.2 UDP-MurNAc-L-Ala-L-Glu ligase assay with XOO_1320

To investigate whether XOO_1320 had the predicted UDP-MurNAc-L-Ala-L-Glu ligase activity, recombinant XOO_1320 was incubated with UDP-MurNAc-L-Ala and L-Glu. By LC-MS analysis, I detected large amounts of a new product (100 times that produced with D-Glu, Figure 2.12). This new product had the same mass spectrum as UDP-MurNAc-L-Ala-D-Glu (Figure 2.13), but two compounds had different retention time. Consequently, this new product was proposed to be UDP-MurNAc-L-Ala-L-Glu.

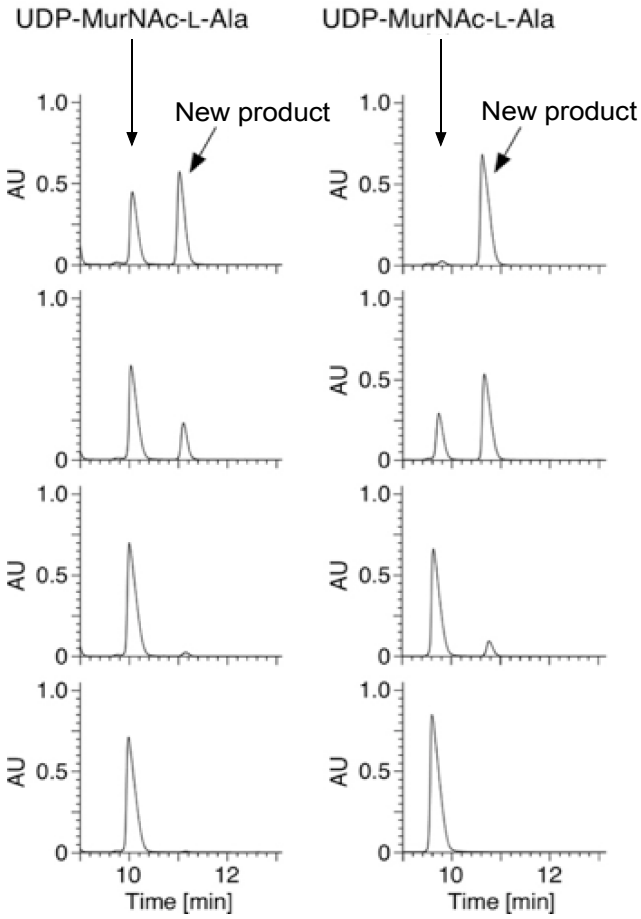

Figure 2.12 Glu ligase assay with recombinant XOO_1320 using L-Glu as a substrate.
HPLC traces of the reaction products formed with 50, 17, and 5.6 μg mL^{-1} (0.96, 0.32, and 0.11 μM) of XOO_1320 and boiled XOO_1320 (from top to bottom) after 5 min (left column) and 2 h (right column) reaction times are shown.

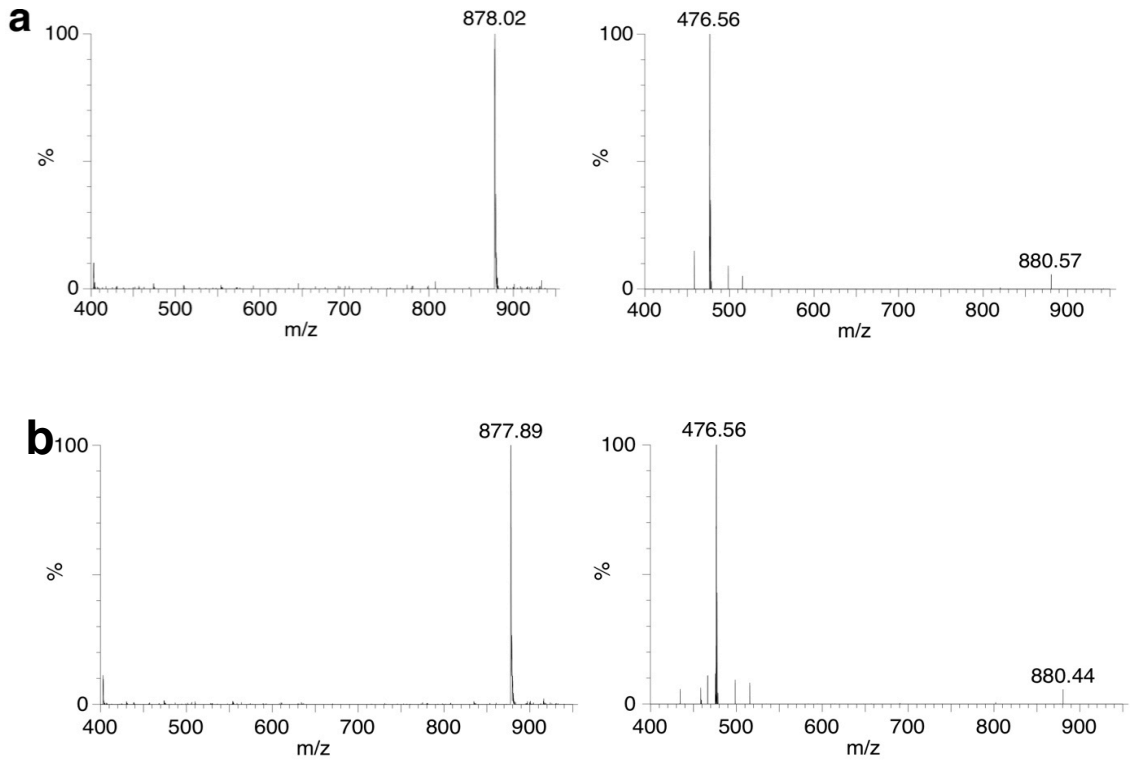

Figure 2.13 MS spectra of UDP-MurNAc-L-Ala-Glu formed by recombinant XOO_1320 and MurD.
(a) MS spectra of the product formed from UDP-MurNAc-L-Ala and L-Glu with recombinant XOO_1320 (left, ESI negative mode; right, ESI positive mode) are shown. Furthermore, based on HR-ESI-FT-MS analysis (m/z: $[M-H]^-$ calculated for $C_{28}H_{42}O_{23}N_5P_2$, 878.17513; observed, 878.17735), the molecular formula of the product was determined to be $C_{28}H_{43}O_{23}N_5P_2$. (b) Mass spectra of the UDP-MurNAc-L-Ala-D-Glu (left, ESI negative mode; right, ESI positive mode).

To confirm whether this new product was the proposed UDP-MurNAc-L-Ala-L-Glu, the chirality of the Glu moiety of the product was then analyzed by the same method as described above. LC-MS analysis revealed that the reaction product included only L-Glu (Figure 2.14). Consequently, this new product was proved to be UDP-MurNAc-L-Ala-L-Glu, clearly showing that XOO_1320 was the other type of MurD utilizing L-Glu as the main substrate.

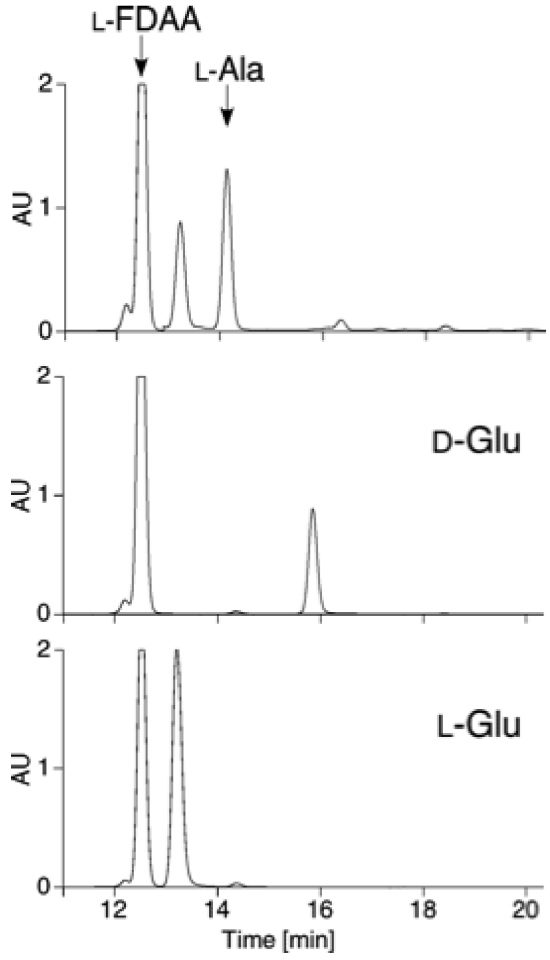

Figure 2.14 Chiral analysis of the terminal Glu residue of the reaction product formed from UDP-MurNAc-L-Ala and L-Glu by recombinant XOO_1320 (upper).
L-FDAA derivative of Glu released by acid hydrolysis of the reaction product was analyzed by HPLC with detection at UV 340 nm. The standards, D-Glu (middle) and L-Glu (lower), were also analyzed.

2.3.2.4.3 Glu epimerase assay with XOO_1319

I next examined whether XOO_1319 had predicted glycopeptidyl-glutamate epimerase activity. In this assay, recombinant XOO_1319 was incubated with enzymatically synthesized and purified UDP-MurNAc-L-Ala-L-Glu under various conditions.

When the enzyme was incubated with the substrate in the presence of ATP and Mg^{2+}, a new product was detected. This new product had the same elution time as the standard UDP-MurNAc-L-Ala-D-Glu (Figure 2.15). Moreover, this new product had the same mass spectrum as UDP-MurNAc-L-Ala-D-Glu (Figure 2.16), suggesting this new product was UDP-MurNAc-L-Ala-D-Glu.

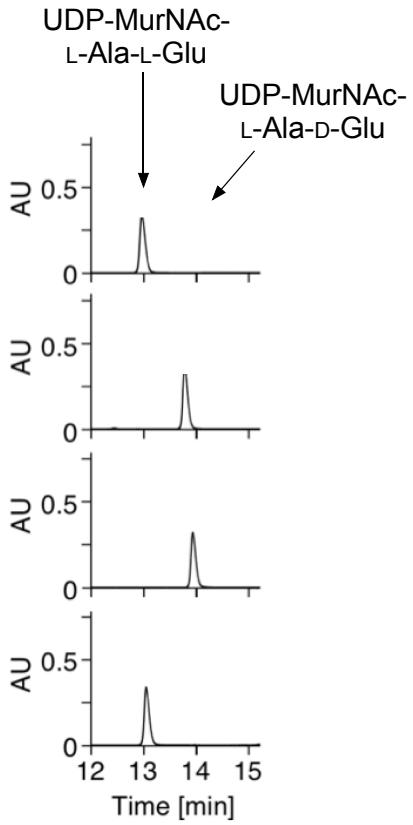

Figure 2.15 UDP-MurNAc-L-Ala-L-Glu epimerase activity of recombinant XOO_1319.
Boiled (top) or active enzyme (second) was used for the *in vitro* assay. HPLC traces of the reaction products are shown. Enzymatically prepared UDP-MurNAc-L-Ala-D-Glu (third) and UDP-MurNAc-L-Ala-L-Glu (bottom) were also analyzed.

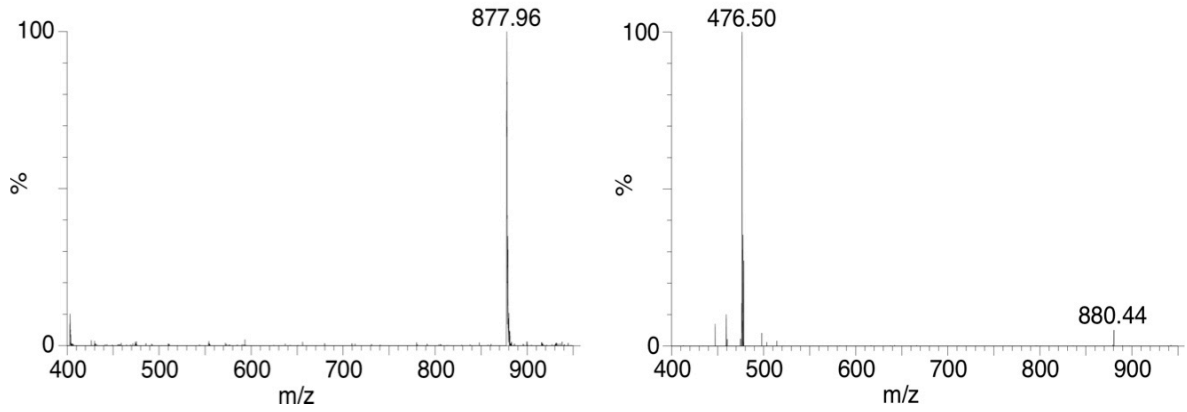

Figure 2.16 MS spectra of the product formed from UDP-MurNAc-L-Ala-L-Glu with recombinant XOO_1319

left, ESI negative mode; right, ESI positive mode. Furthermore, based on HR-ESI-FT-MS analysis (m/z: $[M-H]^-$ calculated for $C_{28}H_{42}O_{23}N_5P_2$, 878.17513; observed, 878.17764), the molecular formula of the product was determined to be $C_{28}H_{43}O_{23}N_5P_2$.

To confirm whether this new product was the proposed UDP-MurNAc-L-Ala-D-Glu, the chirality of the Glu moiety of the product was then analyzed by the same method as described above. LC-MS analysis revealed that the reaction product included only D-Glu (Figure 2.17). Consequently, this new product was proved to be UDP-MurNAc-L-Ala-D-Glu, clearly showing that XOO_1319 was a novel type of glycopeptidyl-glutamate epimerase.

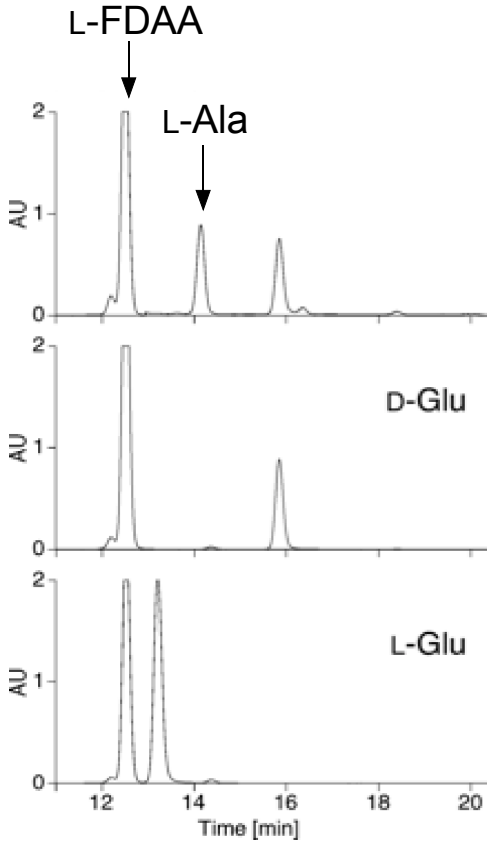

Figure 2.17 Chiral analysis of the terminal Glu residue of the reaction product formed from UDP-MurNAc-L-Ala-L-Glu by recombinant XOO_1319 (upper).
L-FDAA derivative of Glu released by acid hydrolysis of the reaction product was analyzed by HPLC with detection at UV 340 nm. The standards, D-Glu (middle) and L-Glu (lower), were also analyzed.

2.3.3 Biochemical characterization of XOO_1319

2.3.3.1 Substrate activation mechanism

As mentioned before, ATP is necessary for XOO_1319 epimerase reaction. To understand the substrate-activation mechanism of XOO_1319, the formation of AMP or ADP after the reaction was investigated. LC-MS analysis revealed that only AMP was formed (Figure 2.18), suggesting that the substrate was perhaps activated by adenylation.

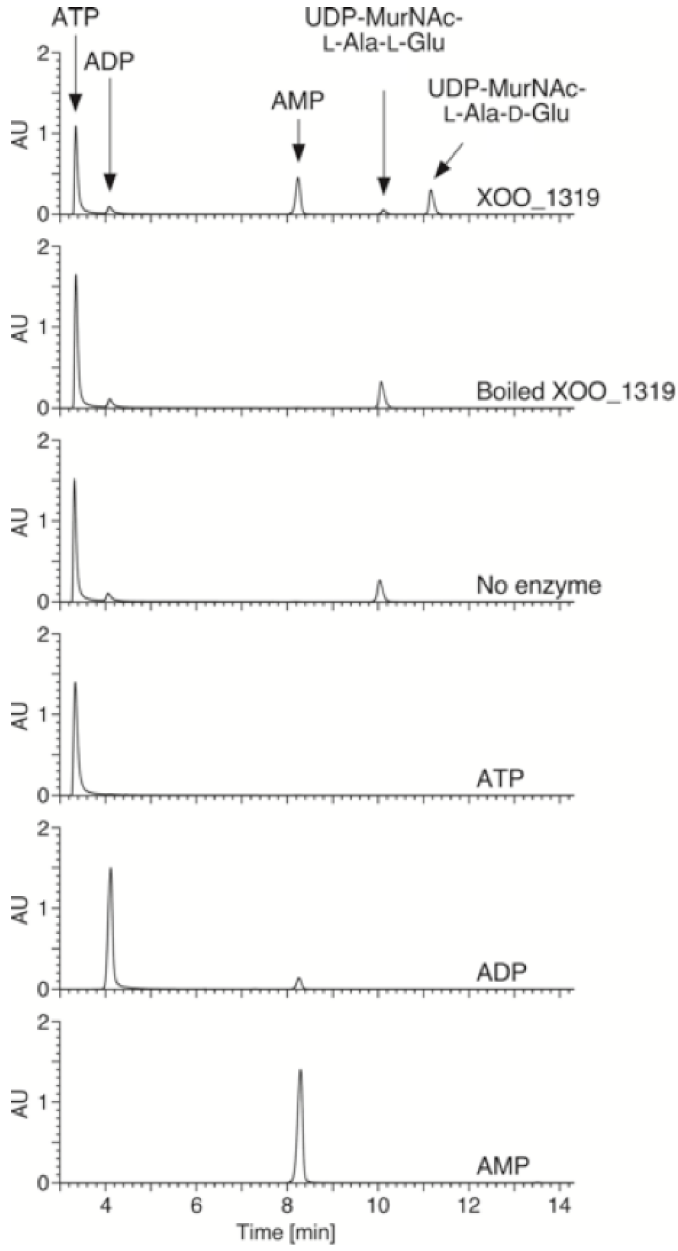

Figure 2.18 Substrate-activation mechanism of XOO_1319.
HPLC traces of the reaction products formed with XOO_1319 under the reaction conditions (100 mM Tris-HCl buffer (pH 8.0), 1 mM UDP-MurNAc-L-Ala-L-Glu, 1 mM ATP, and 20 mM $MgCl_2$) with 20 μg mL^{-1} (0.39 μM) of purified recombinant XOO_1319 (top), boiled XOO_1319 (second), and no enzyme (third) are shown. The standards, 1 mM of ATP (fourth), ADP (fifth), and AMP (bottom), were also analyzed.

2.3.3.2 Reverse reaction

To examine whether XOO_1319 could catalyze the reverse reaction with UDP-MurNAc-L-Ala-D-Glu as the substrate, I incubated the enzyme with UDP-MurNAc-L-Ala-D-Glu in the presence of ATP and Mg^{2+}. However, no epimerase activity was detected (Figure 2.19), suggesting that only UDP-MurNAc-L-Ala-L-Glu can be activated by the enzyme with ATP.

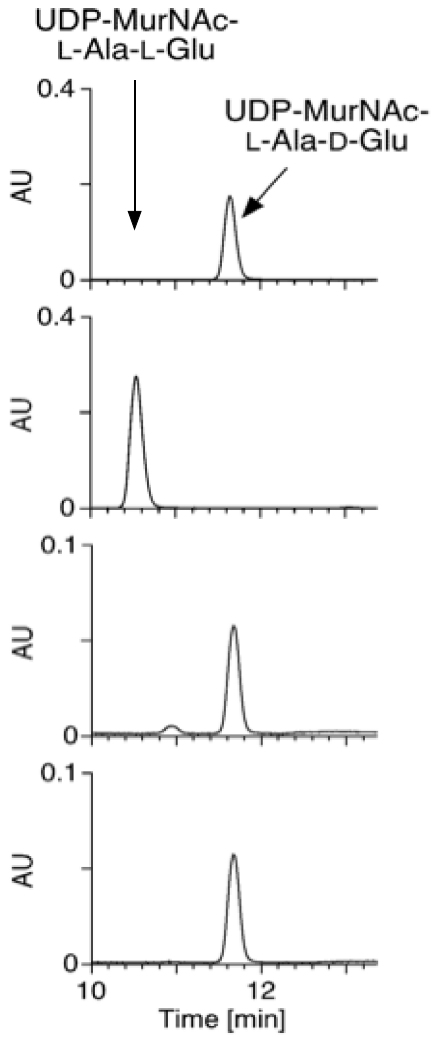

Figure 2.19 UDP-MurNAc-L-Ala-D-Glu epimerase activities with recombinant XOO_1319.
HPLC traces of the standard UDP-MurNAc-L-Ala-D-Glu, standard UDP-MurNAc-L-Ala-L-Glu, the reaction products using UDP-MurNAc-L-Ala-D-Glu as the substrate with XOO_1319 or boiled XOO_1319 are shown (from top to bottom)

2.3.4 Orthologs of XOO_1319 and XOO_1320

2.3.4.1 Occurrence of XOO_1319 orthologs among bacteria

Most orthologs of XOO_1319 and XOO_1320 exist next to each other in the genome. I investigated the occurrence of XOO_1319 orthologs among bacteria and found the orthologs exist in Gammaproteobacteria including the genera *Stenotrophomonas*, *Dyella*, *Frateuria*, *Rhodanobacter*, *Pseudoxanthomonas*, and *Lysobacter* besides *Xanthomonas* and *Xylella*. Several rare actinobacteria such as the genera *Micromonospora*, *Actinoplanes*, *Verrucosispora*, and *Salinispora* also possess orthologs. Moreover, I detected orthologs in a few strains belonging to Alphaproteobacteria including the genera *Devosia*, *Pelagibacterium*, and *Parvularcula*. Orthologs with low similarity are found in a plant pathogenic fungus (*Phytophthora sojae*), cyanobacteria (*Anabaena* sp. and *Cylindrospermum stagnale*), and an amoeba (*Acanthamoeba castellanii*) (Table 2.2).

Table 2.2. Orthologs of XOO_1319 and XOO_1320.

Strains	XOO_1319		XOO_1320	
	Genes	Identity (%)	Genes	identity (%)
Gammaproteobacteria				
Xanthomonas campestris	XCC2739	89	XCC2738	86
Xylella fastidiosa	XF_1117	78	XF_1118	70
Stenotrophomonas maltophilia	Smlt1169	80	Smlt1170	73
Dyella japonica	HY57_07395	60	HY57_07400	51
Frateuria aurantia	Fraau_2759	61	Fraau_2758	49
Rhodanobacter denitrificans	R2APBS1_3190	59	R2APBS1_3189	53
Pseudoxanthomonas spadix	DSC_05870	70	DSC_05875	67
Lysobacter antibioticus	LA76x_1651	78	LA76x_1652	66
Actinobacteria				
Micromonospora sp.	ML5_4079	44	ML5_4080	38
Actinoplanes sp.	ACPL_1937	43	ACPL_1938	37
Verrucosispora maris	VAB18032_25495	45	VAB18032_25490	37
Salinispora tropica	Strop_3006	42	Strop_3005	39
Alphaproteobacteria				
Devosia sp. H5989	XM25_12455	40	XM25_12460	34
Pelagibacterium halotolerans	KKY_2207	41	KKY_2208	33
Parvularcula bermudensis	PB2503_10394	38	PB2503_10389	33
Cyanobacteria				
Anabaena sp.	AA650_10885	25	AA650_08185	28
Cylindrospermum stagnale	Cylst_2487	25	Cylst_2103	28
Fungus				
Phytophthora sojae	PHYSODRAFT_561587	29	none	
Amoeba				
Acanthamoeba castellanii	ACA1_115170	30	none	

Identity was analyzed using BLAST search (http://www.genome.jp/tools/blast/) of the protein sequences.

2.3.4.2 Function analysis of XOO_1319 and XOO_1320 orthologs

2.3.4.2.1 Preparation of recombinant enzymes of XOO_1319 and XOO_1320 orthologs

To confirm whether the orthologs had the same activities as XOO_1319 and XOO_1320, I prepared recombinant enzymes of orthologs found in a *Micromonospora* strain, a *Salinispora* strain, and a *Stenotrophomonas maltophilia* strain.

The obtained recombinant enzymes MCAG_01009, MCAG_01010 from *Micromonospora* sp., Strop_3005, Strop_3006 from *S. Tropica,* and DP16_1118, DP16_1119 from *S.maltophilia* were subjected to SDS-PAGE analysis to confirm the molecular size and purity (Figure 2.20). Then the enzymes were used for in vitro experiments.

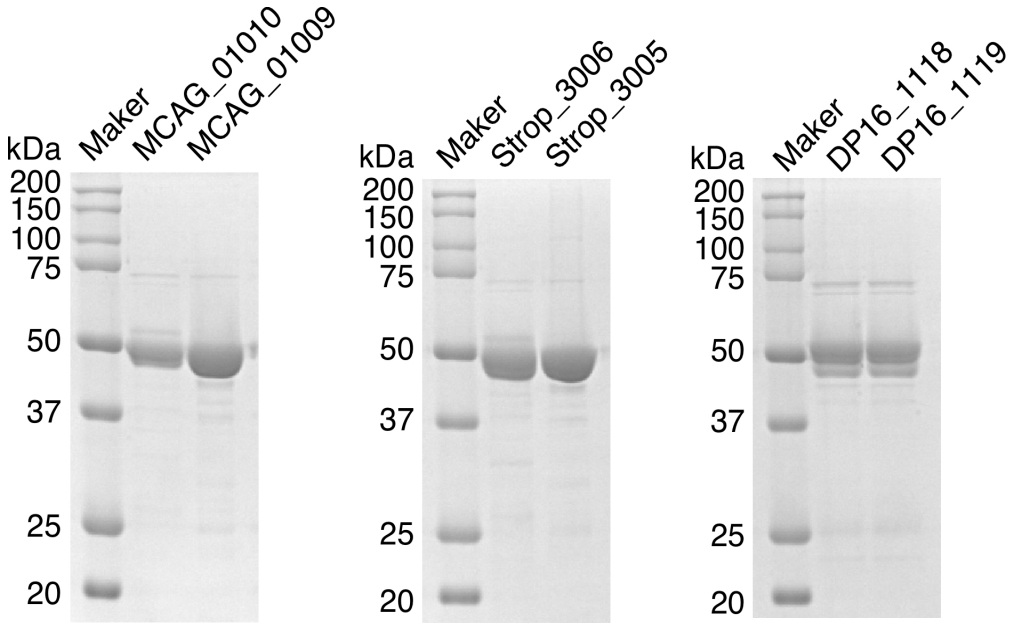

Figure 2.20 Expression and purification of recombinant MCAG_01009, MCAG_01010, Strop_3005, Strop_3006, DP16_1118, and DP16_1119.
SDS-PAGE analysis of purified MCAG_01009 (49.8 kDa), MCAG_01010 (50.4 kDa), Strop_3005 (49.1 kDa), Strop_3006 (51.2 kDa), DP16_1118 (51.9 kDa), and DP16_1119 (52.0 kDa).

2.3.4.2.2 L-Glu ligase assay with XOO_1320 orthologs

To check whether XOO_1320 orthologs had UDP-MurNAc-L-Ala-L-Glu ligase activity, Strop_3005 from *S. tropica*, MCAG_01009 from *Micromonospora* sp., and DP16_1119 from *S. maltophilia* were incubated with UDP-MurNAc-L-Ala and L-Glu under the same conditions as described above. LC-MS analysis revealed that XOO_1320 orthologs had L-Glu ligase activity (Figure 2.21).

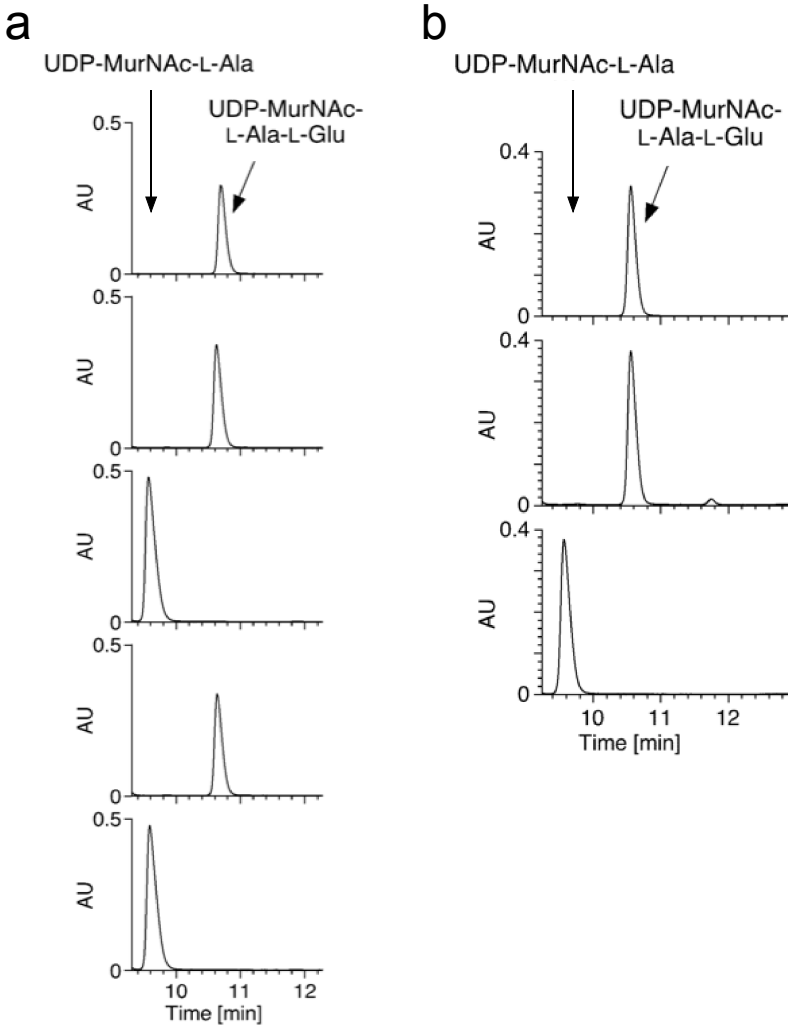

Figure 2.21 UDP-MurNAc-L-Ala-L-Glu ligase activities of XOO_1320 orthologs. (a) HPLC trace of the standard of UDP-MurNAc-L-Ala-L-Glu, reaction products with Strop_3005, boiled Strop_3005, MCAG_01009, or boiled MCAG_01009 are shown (from top to bottom). (b) HPLC trace of the standard UDP-MurNAc-L-Ala-L-Glu, the reaction products with DP16_1119, or boiled DP16_1119 are shown (from top to bottom)

2.3.4.2.3 Glu epimerase assay with XOO_1319 orthologs

To check whether XOO_1319 orthologs had Glu epimerase activity, Strop_3006 from *S. tropica*, MCAG_01010 from *Micromonospora* sp., and DP16_1118 from *S. maltophilia* were incubated with UDP-MurNAc-L-Ala-L-Glu in the presence of ATP and Mg^{2+}. LC-MS analysis revealed that XOO_1319 orthologs had Glu epimerase activity (Figure 2.22).

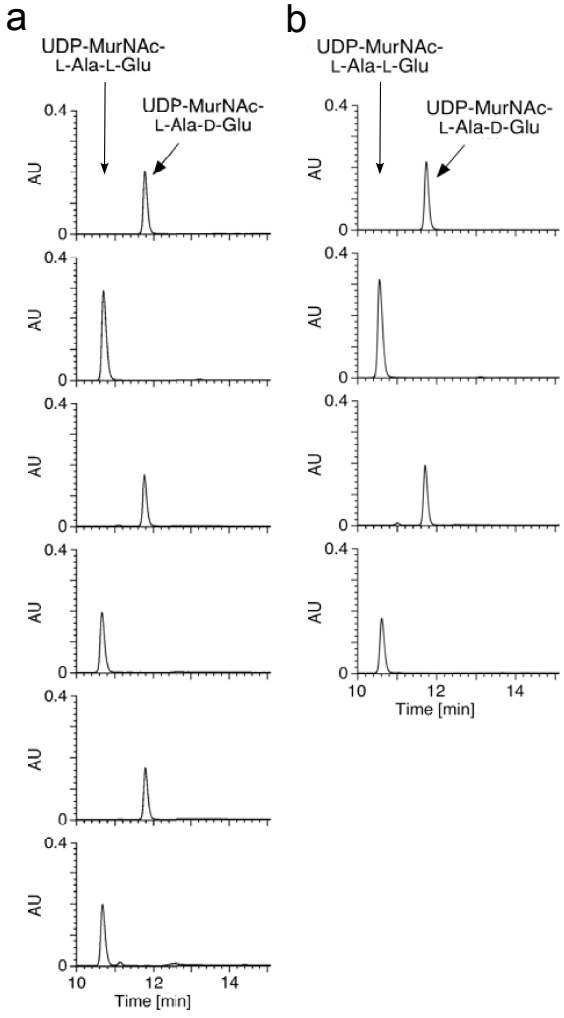

Figure 2.22 Glu epimerase activities of XOO_1319 orthologs.
(a) HPLC traces of the standard of UDP-MurNAc-L-Ala-D-Glu, the standard of UDP-MurNAc-L-Ala-L-Glu, the reaction products with Strop_3006, boiled Strop_3006, MCAG_01010, or boiled MCAG_01010 are shown (from top to bottom).
(b) HPLC traces of the standard of UDP-MurNAc-L-Ala-D-Glu, the standard of UDP-MurNAc-L-Ala-L-Glu, the reaction products with DP16_1118, or boiled DP16_1118, are shown (from top to bottom).

2.4 Discussion

In this chapter, I revealed that a different peptidoglycan biosynthetic pathway is operating in *X. oryzae* and that two enzymes, XOO_1320 and XOO_1319, catalyze the ligation of L-Glu to UDP-MurNAc-L-Ala and the epimerization of the terminal L-Glu of the product, respectively.

The XOO_1319 and XOO_1320 orthologs also exist in some microorganisms, and I confirmed that the orthologs from *Micromonospora* sp., *Salinispora tropica* and *Stenotrophomonas maltophilia* had the same activities. Based on these results, the novel Glu epimerase XOO_1319 was renamed to MurL and UDP-MurNAc-L-Ala-L-Glu synthetase XOO_1320 was renamed to MurD2 (Figure 2.23).

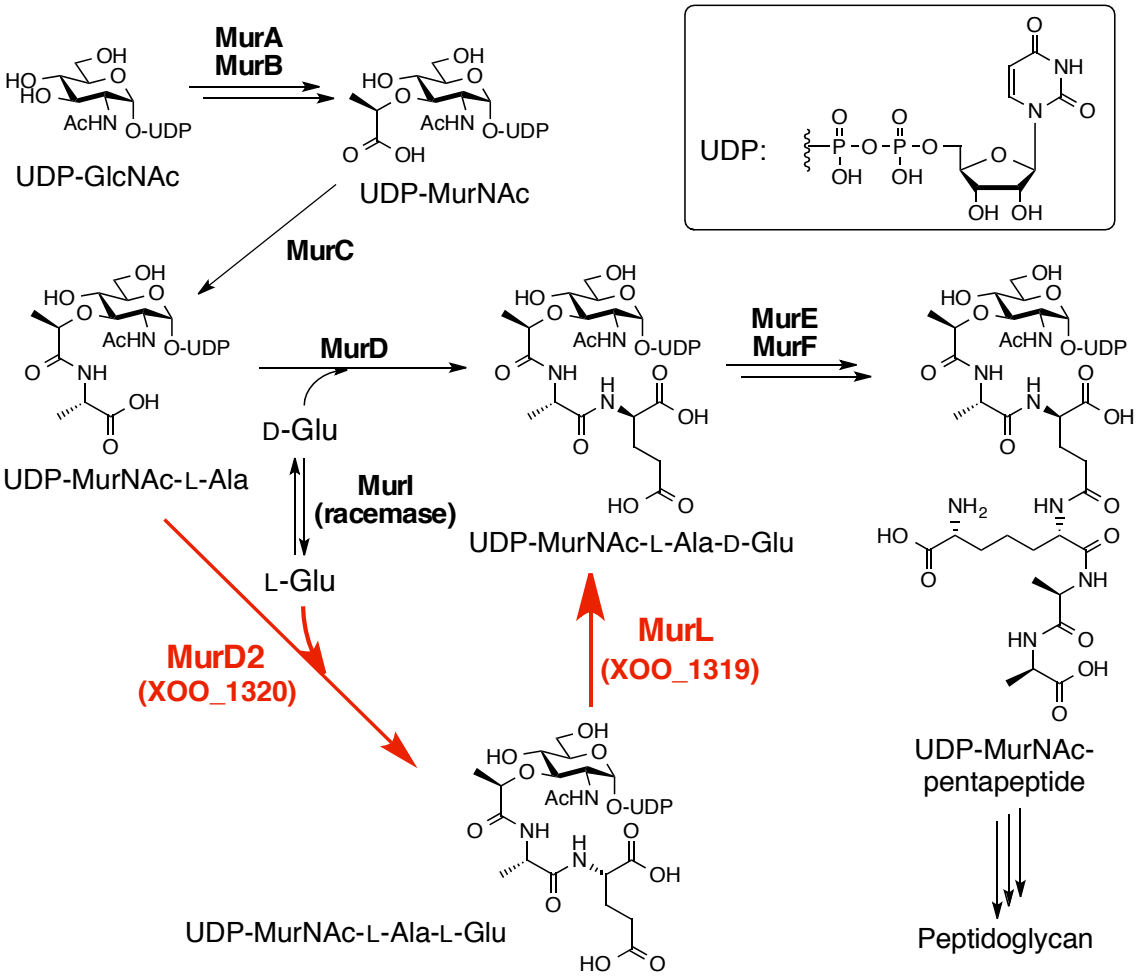

Figure 2.23 Peptideglycan biosynthetic pathways of MurD/MurI and MurD2/MurL.

MurL is the first example of an epimerase using ATP as the cofactor. MurL has no conserved domains or co-factor binding domains, making it difficult to estimate the exact reaction mechanism of the enzyme. To understand the epimerization mechanism of MurL, Prof. H. Morita (Toyama University) tried to solve the crystal structure of the enzyme using MurL ortholog from *S. maltophilia*. Recently, some amino acid residues were suggested to be responsible for epimerase activity based on the incomplete crystal structure analysis. To confirm the function of these residues, the residues were replaced with other amino acids and the mutated enzymes were used for epimerase assay. As a result, His210, Lys259, and Lys331 were confirmed to be necessary for epimerase activity. The single mutants of these residues completely lost the epimerase activity.

Based on these observations, Prof. H. Morita estimated the structure of MurL and a reaction mechanism of MurL was proposed (Figure 2.24). Considering that electron-withdrawing property of a phosphate group increase the acidity of alpha-proton of the glutamate acid moiety, the reaction might start with adenylation of the alpha carboxyl group. Under the reaction conditions (pH=8), His210 will act as a base to abstract a proton from Lys259. Since Lys259 is located far from His210, there might be another important residue between His210 and Lys259 to form an activation worknet. Next, Lys259 abstracts alpha-proton from L-Glu and Lys331 might provide a proton in the opposite direction. Then the hydrolysis of AMP will give final product. The structure model is consistent with the observation that the reaction is irreversible since UDP-MurNAc-L-Ala-D-Glu could not enter the active site of the enzyme.

However, at this stage, it is difficult to predict the detailed reaction mechanism. A complete crystal structure analysis is necessary in the future work.

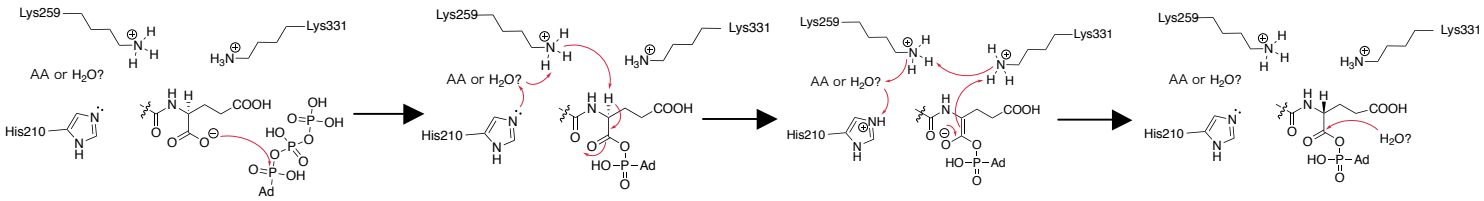

Figure 2.24 Proposed reaction mechanism of MurL

Chapter 3

Amino acid residues recognizing isomeric glutamate substrates in MurD2 and MurD

3.1 Introduction

In chapter 2, I characterized MurD2 of *X. oryzae*, which catalyzes the ligation of L-Glu to UDP-MurNAc-L-Ala. The MurD2 possesses 26% identity with $MurD_{ec}$ of *E. coli*, even though $MurD_{ec}$ ligates D-Glu to UDP-MurNAc-L-Ala. Since MurD2 and $MurD_{ec}$ are attractive potential drug targets, the isomer recognition mechanism of these two enzymes may provide some clues for drug discovery and design. In this work, I explored the isomer recognition mechanism of the enzymes.

To understand how *X. oryzae* MurD2 recognizes the isomer substrate, Prof. H. Morita (Toyama University) estimated the structure of MurD2 of *X. oryzae* based on the structure of $MurD_{ec}$ (9, 28-33) during docking simulations. Based on the structure models, I found some candidate amino acid residues, which are perhaps responsible for L-Glu recognition. To confirm the function of these residues in MurD2, I employed the site-direct mutagenesis to replace the residues with their corresponding amino acid residues in $MurD_{ec}$. Consequently, I obtained a mutated MurD2 enzyme that contained two amino acid substitutions and accepted only D-Glu as the substrate.

Also, a previous work reported that $MurD_{ec}$ had a very strict substrate specificity (9). To further study the substrate specificity of $MurD_{ec}$, I tried to convert the substrate specificity of $MurD_{ec}$ using the same strategy, but the mutant enzyme still accepted only D-Glu. Then, MurD of *Streptococcus mutans* ($MurD_{sm}$), which possesses the key amino acid residue for L-Glu recognition identified in MurD2, was used for random screenings of mutant enzymes accepting L-Glu. Consequently, I obtained a mutated $MurD_{sm}$ that had one amino acid substitution and slightly accepted L-Glu. A mutated $MurD_{ec}$ possessing the corresponding one amino acid substitution also accepted L-Glu.

Thus, I revealed that a few amino acid residues in MurD/MurD2 might control the acceptability of substrates with different stereochemistries.

In this chapter, the details of these experiments are described.

3.2 Materials and methods

3.2.1 Strain

Genomic DNA of *Streptococcus mutans* NBRC13955 was obtained from National Institute of Technology and Evaluation (Tokyo, Japan). LB broth media was used for liquid cultivation.

3.2.2 Plasmid construction

Primers used for plasmid construction were summarized in Table 3.1

3.2.2.1 Construction of mutants of MurD2 and $MurD_{ec}$

DNA fragment carrying E197D, R358K, P433A and F435L mutations in MurD2 were amplified by overlap extension PCR with appropriate primers using pET28-MurD2 as the template. As for construction of E197D/R358K double mutant of MurD2, pET28-MurD2_R358K was used as the template. The DNA fragments digested with *Nde*I/*Hin*dIII were inserted into the same sites of the pET28a. DNA fragments carrying D182E, K348R, A414P, L416F, and K319T mutations in $MurD_{ec}$ were amplified by overlap extension PCR with appropriate primers using pQE80-$MurD_{ec}$ as the template. As for construction of D182E/K348R double mutant of $MurD_{ec}$, pQE80-$MurD_{ec}$_K348R was used as the template. The DNA fragments digested with *Bam*HI/*Hin*dIII were inserted into the same sites of pQE80.

3.2.2.2 Construction of pET28-$MurD_{sm}$

DNA fragment containing $murD_{sm}$ of *S. mutans* NBRC13955 was amplified by overlap extension PCR with appropriate primers and the genomic DNA as template to

erase the *Nde*I site at 546 bp. The amplified fragment digested with *Nde*I/*Bam*HI was inserted into the same sites of the pET28a.

3.2.2.3 Construction of mutants of MurDsm

DNA fragment carrying T192E mutation in $MurD_{sm}$ was amplified by overlap extension PCR with appropriate primers using pET28-$MurD_{sm}$ as template. The DNA fragments digested with *Nde*I/*Bam*HI were inserted into the same sites of the pET28a. DNA fragment carrying K330T in $MurD_{sm}$ was amplified with appropriate primers using pSTVL– $MurD_{sm}$_K330T as template. The fragment digested with *Nde*I/*Bam*HI was inserted into the same sites of pET28a.

3.2.2.4 Construction of pSTVL

DNA fragment containing *murL* of *X. oryzae* MAFF311018 was amplified by PCR using gene-specific primers. The DNA fragment digested with *Nde*I/*Hin*dIII was inserted into the same sites of pSTV28N to construct pSTVL.

3.2.2.5 Construction of pSTVL–$MurD_{sm}$

DNA fragment containing $murD_{sm}$ was amplified by overlap extension PCR with appropriate primers and pET28-$MurD_{sm}$ as template to erase the *Hin*dIII site at 1,020 bp. The DNA fragment digested with *Hin*dIII was inserted into the same site of pSTVL.

3.2.2.6 Construction of pSTVL–MurD$_{ec}$

DNA fragment containing *murD*$_{ec}$ was amplified by PCR using gene-specific primers. The DNA fragment digested with *Hin*dIII was inserted into the same sites of pSTVL.

3.2.2.7 Construction of mutants of pSTVL–MurD$_{ec}$

DNA fragment carrying K319T and K319I mutations in MurD$_{ec}$ were amplified by overlap extension PCR with appropriate primers using pQE80-MurD$_{ec}$ as the template. As for construction of D182E/K319T, K319T/K348R, D182E/K319I, and K319I/K348R double mutants of MurD$_{ec}$, pQE80-MurD$_{ec}$_D182E or pQE80-MurD$_{ec}$_K348R was used as the template. As for construction of D182E/K319T/K348R and D182E/K319I/K348R triple mutants of MurD$_{ec}$, pQE80-MurD$_{ec}$_D182E/K348R was used as the template. The DNA fragments digested with *Bam*HI/*Kpn*I were inserted into the same sites of pSTVL–MurD$_{ec}$.

Table 3.1 Primers used for plasmid construction

Primers Sequences (5' to 3')
For pET28-MurD2_E197D construction
AATCTATTTCCCGATCATCTGGACTGGCACGGCGAT
GTGCCAGTCCAGATGATCGGGAAATAGATTCAACACCACC
ATAGAATTCTTAAGAAGGAGATATACATATGCGAATTTCGCAGTTTGAAGGCAAGG
AGTAAGCTTAATGCACACCCAACCCGGGAATCG
For pET28-MurD2_R358K construction
TCGGCGGGCACGACAAAGGCCTGGACTGGCACGATT
GTGCCAGTCCAGGCCTTTGTCGTGCCCGCC
For pET28-MurD2_P433A construction
GCGGCCAGCTTCGGCGCCTATAGCGACTACGTT
GCCGAAGCTGGCCGCCCCCGGCGAGAGCA
For pET28-MurD2_F435L construction
CCAGCCTGGGCGCCTATAGCGACTACGTT
TAGTCGCTATAGGCGCCCAGGCTGGGCGCCCCCGGCGAGAG
For pQE80-MurD$_{ec}$_D182E construction
TGACTGAAGAGCATATGGATCGCTATCCGTTTGGTTTA
CGATCCATATGCTCTTCAGTCACGTTCAGAATGGTC
TATGGATCCGCTGATTATCAGGGTAAAAATGTCGTCATTATCGG
TATAAGCTTCAACCTAACTCCTTCGCCAGACGGGCAAAC
For pQE80-MurD$_{ec}$_K348R construction
GTGGCGATGGTCGCTCGGCGGACTTTAGCCCA
TAAAGTCCGCCGAGCGACCATCGCCACCCAGCAACAAAT
For pQE80-MurD$_{ec}$_A414P construction
CCCCAGCCTGTCCGAGCCTTGATCAGTTCAAGAACTT
CTGATCAAGGCTCGGACAGGCTGGGGAGAGCAGAACCA
For pQE80-MurD$_{ec}$_ L416F construction
CCCAGCCTGTGCCAGCTTCGATCAGTTCAAGAACTTTG
AACTGATCGAAGCTGGCACAGGCTGGGGAGAGCAGAAC
For pQE80-MurD$_{ec}$_K319T construction
GATTAACGATTCGACCGCGACCAACGTCGGCAGTACG
GACGTTGGTCGCGGTCGAATCGTTAATCCAACG
For pET28-MurD$_{sm}$ construction

GAGATAAACATATGAAACACGTCAAAAATTTTGAAAATAAAAAGGTTTTGGTTC
CGGAAAGTTTTCATCCGCACATGGCAGTGATTACCAATTTGATGC
GGTAATCACTGCCATGTGCGGATGAAAACTTTCCGTTCCCATCAATTG
ATAGGATCCTATTCTCCTTTAAGGGACTTAAAAGTTGTGATAAATTCATCTCC

For pET28-MurD$_{sm}$_T192E construction
AATTTGATGCCAGAACATATTGACTATCATGGTTCAT
GATAGTCAATATGTTCTGGCATCAAATTGGTAATCACTG

For pET28-MurD$_{sm}$_K330T construction
GAGATAAACATATGAAACACGTCAAAAATTTTGAAAATAAAAAGGTTTTGGTTC
ATAGGATCCTATTCTCCTTTAAGGGACTTAAAAGTTGTGATAAATTCATCTCC

For pSTVL construction
ATAGAATTCTTAAGAAGGAGATATACATATGAGCGCTTTCGACAAACATCAGATTTCC
TATAAGCTTCTAGCCTTCAAACTGCGAAATTCGCACGCAC

For pSTVL–MurD$_{sm}$ construction
GTTTAAGCTTAAGAAGGAGATATACCATGGGCAGCAGCCATC
TTATCAAATCCTGACAACGCTTTTTGAGTGGCTAAAATATTGGTTGAC
TTTAGCCACTCAAAAAGCGTTGTCAGGATTTGATAATAGCAAGGT
GCTAGTTATTGCTCAGCGGTGG

For pSTVL-MurD$_{ec}$ construction
GAGAAGCTTAAAGAGGAGAAATTAACTATGAGAGGATCGCATCACC
TATAAGCTTGGTACCTCAACCTAACTCCTTCGCCAGACGGGCAAAC

For pSTVL-MurD$_{ec}$-K319I construction
TATGGATCCGCTGATTATCAGGGTAAAAATGTCGTCATTATCGG
TATAAGCTTGGTACCTCAACCTAACTCCTTCGCCAGACGGGCAAAC
GATTAACGATTCGATTGCGACCAACGTCGGCAGTACG
GACGTTGGTCGCAATCGAATCGTTAATCCAACG

For pSTVL-MurD$_{ec}$-K319T construction
GATTAACGATTCGACCGCGACCAACGTCGGCAGTACG
GACGTTGGTCGCGGTCGAATCGTTAATCCAACG

Underlining indicates restriction enzyme sites or mutated codons

3.2.3 In vitro assay

E. coli BL21(DE3) harboring the recombinant expression plasmids was grown in LB medium (1 L) supplemented with Ap or Km. Culture condition and protein purification procedures were essentially the same as those described in the materials and methods **2.2**. A reaction mixture (100 μL) containing 100 mM Tris-HCl buffer (pH 8.0), 1 mM UDP-MurNAc-L-Ala, 10 mM ATP, 20 mM $MgCl_2$, 2.5 mM 2-mercaptoethanol, 25 mM $(NH_4)_2SO_4$, 5 mM of D-Glu or L-Glu, and 0.39 μM purified recombinant enzymes were incubated at 37°C for 2 h. After heat treatment and centrifugation, the supernatant was subjected to LC-MS analysis. The analytical conditions were described in the materials and methods **2.2**.

3.2.4 Random mutagenesis

The error-prone PCR mixture contained, in a final volume of 100 μl, PCR buffer, 5 mM $MgCl_2$, 200 μM dNTP, 400 μM $MnCl_2$, 0.2 μM primers (Table 3.2), 2 ng pET28-$MurD_{sm}$ plasmid, and 1 U of Platinum Taq polymerase (Thermo Fisher Scientific Inc.). PCR conditions were as follows: 94°C for 2 min followed by 30 cycles of 94°C for 30 sec, 55°C for 30 sec, and 72°C for 2 min. The product was digested with *Afl*II/*Bam*HI and inserted into the same sites of pSTVL–$MurD_{sm}$ to replace the parental gene with the mutated genes. The mutagenic library was used for complementation assay with *E. coli* WM335. LB plate containing 30 μg mL^{-1} chloramphenicol was used for screening.

Table 3.2 Primers for random mutagenesis

Primers Sequences (5' to 3')
GTTTAAGCTTAAGAAGGAGATATACCATGGGCAGCAGCCATC
CGTCCCATTCGCCAATCCGGATATAGTTCC

Underlining indicates restriction enzyme sites or mutated codons

3.3 Results

3.3.1 Homology models of MurD2

To understand how *X. oryzae* MurD2 recognizes L-Glu, Prof. H. Morita (Toyama University) constructed homology models of *X. oryzae* MurD2 based on the crystal structures of the $MurD_{ec}$ quaternary complex with substrate UDP-MurNAc-L-Ala, ADP and Mg^{2+} (PDB code: 2UAG) and its tertiary complex with product UDP-MurNAc-L-Ala-D-Glu and Mg^{2+} (PDB code: 4UAG) (29), respectively.

3.3.1.1 Overall structure model of MurD2

The homology models of MurD2 adopted the structure of $MurD_{ec}$ consisting of *N*-terminal (residues 5−98), central (residues 99−314), and *C*-terminal (residues 315−458) domains. A part of the central domain forms the ATP and D-Glu recognition sites with the *C*-terminal domain, while a part of the central and *C*-terminal domains construct the UDP-MurNAc-L-Ala and D-Glu recognition site with the *N*-terminal domain (Figure 3.1).

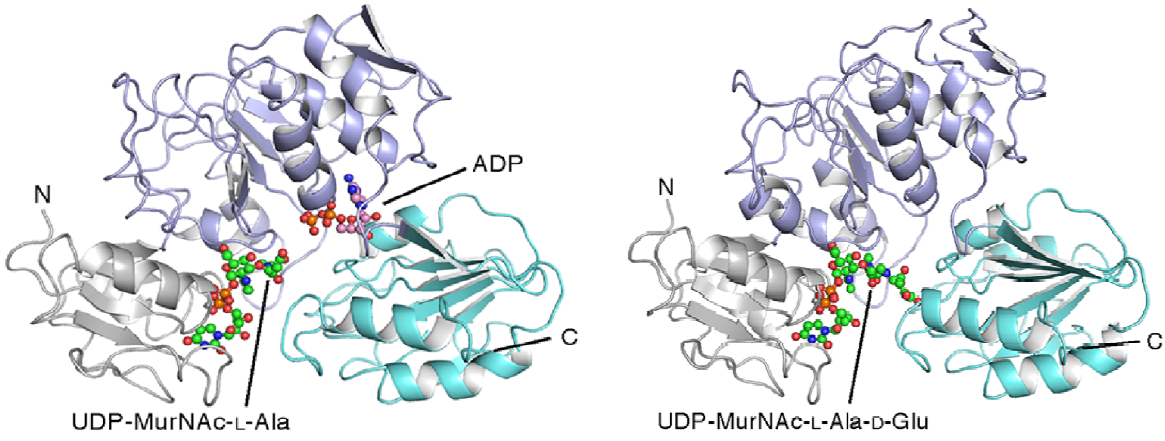

Figure 3.1 Ribbon representations of overall structures of the MurD2 model of the substrate-binding state (left) and its product-binding state (right).
The *N*-terminal, central, and *C*-terminal domains are colored in gray, blue, and cyan, respectively. UDP-MurNAc-L-Ala and ADP bound to the $MurD_{ec}$ quaternary complex structure and UDP-MurNAc-L-Ala-D-Glu bound to the $MurD_{ec}$ tertiary complex structures are shown with the MurD2 models.

3.3.1.2 Comparisons of the active site cavities of MurD2 models with MurD structures

To find important amino acid residues for L-Glu recognition, the active site cavities of the MurD2 models of the substrate-binding state and product-binding state were compared with those of the $MurD_{ec}$ quaternary and tertiary complex structures.

As shown in Figure 3.2, most of the residues lining the ATP, UDP-MurNAc-L-Ala, and D-Glu recognition sites of $MurD_{ec}$ were superimposable on the MurD2 models. However, both MurD2 models of the substrate-binding state and product-binding state suggested that the amino acid residues, Asp182 and Lys348, responsible for the D-Glu recognition in $MurD_{ec}$ were replaced with Glu197 and Arg358, respectively. Moreover, Ala414 and Leu416, located near the D-Glu of the UDP-MurNAc-L-Ala-D-Glu molecule in the $MurD_{ec}$ tertiary complex, were also substituted with Pro433 and Phe435, respectively.

Consequently, I proposed that the unique substrate specificity of MurD2 was caused from alterations among these four residues.

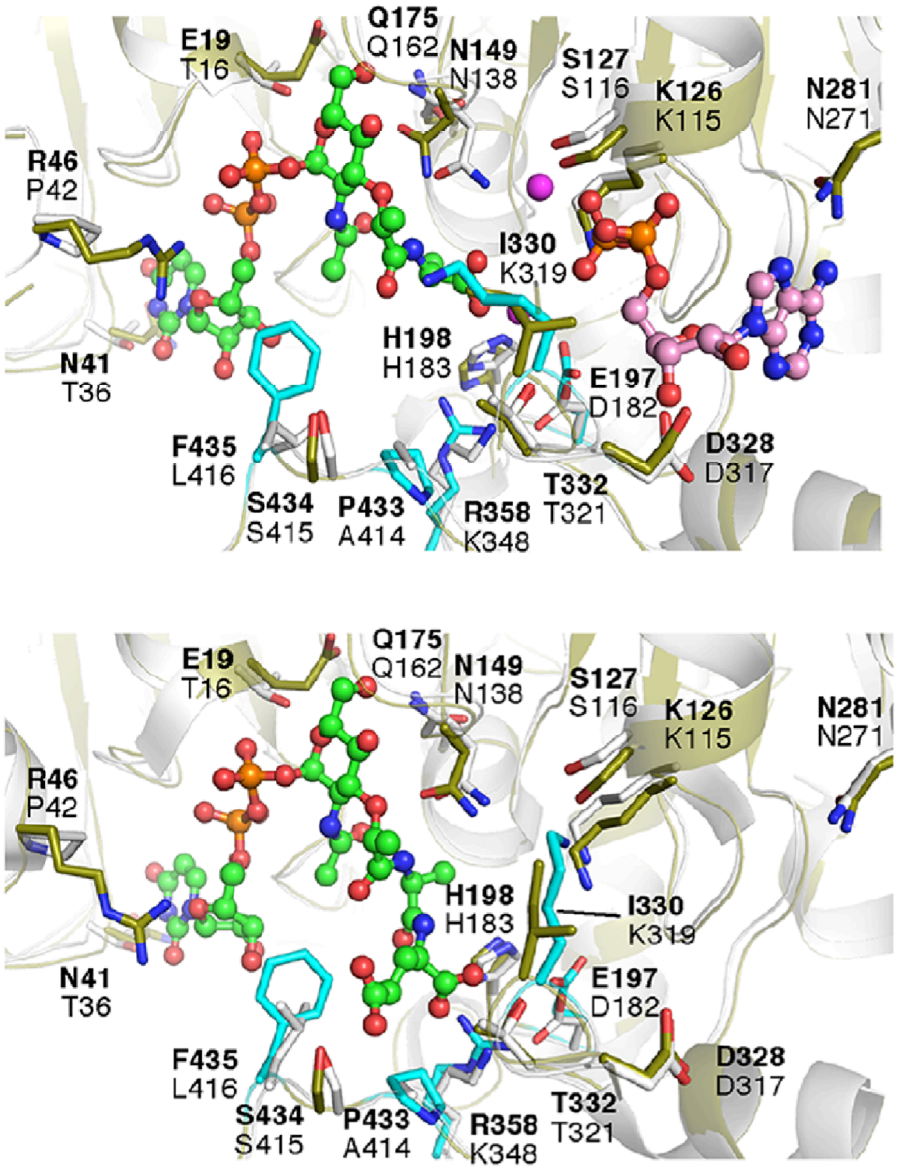

Figure 3.2 Comparisons of the active site cavities of the MurD2 models of the substrate-binding state (top) and its product-binding state (bottom) with those of the $MurD_{ec}$ quaternary and tertiary complex structures, respectively.
The residues of MurD2 and $MurD_{ec}$ are represented with gold and white stick models, respectively, and the residues of MurD2 are indicated with bold numbers. The UDP-MurNAc-L-Ala and UDP-MurNAc-L-Ala-D-Glu molecules are indicated with green ball stick models. The ADP molecule and Mg^{2+} irons are indicated with pink ball stick models and magenta sphere models, respectively. The Glu197, Arg358, Pro433, and Phe435 in MurD2 and Lys319 in $MurD_{ec}$ are indcated with cyan stick models.

3.3.2 Changing the MurD2 substrate specificity

To confirm the function of the candidate amino residues in MurD2, I replaced these residues in MurD2 with their corresponding residues in $MurD_{ec.}$ Then the mutants were used for in vitro experiments to check whether the substrate specificity was changed.

3.3.2.1 Preparation of recombinant enzymes of MurD2 mutants

His-tagged recombinant enzymes of MurD2 mutants were successfully expressed in a soluble form. The obtained recombinant enzymes of were subjected to SDS-PAGE analysis to confirm the molecular size and purity (Figure 3.3).

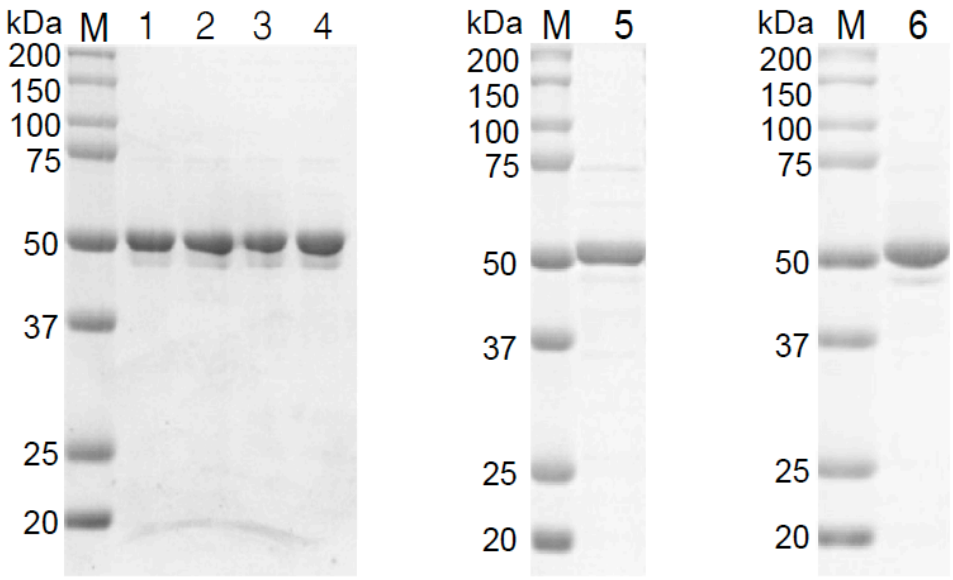

Figure 3.3 SDS-PAGE analysis of purified recombinant MurD2 and its mutants (51.9 kDa).
M, marker; 1, wild type; 2, E197D; 3, R358K; 4, E197D/R358K; 5, P433A; 6, F435L

3.3.2.2 In vitro experiments with MurD2 mutants

To check whether the substrate specificity was changed, the mutants were used for Glu ligase assay using L-Glu or D-Glu as the substrate.

As shown in Figure 3.4, P433A- and F435L-mutated enzymes showed the same activity as that of wild-type MurD2, suggesting that P433 and F435 are not important for MurD2 substrate recognition.

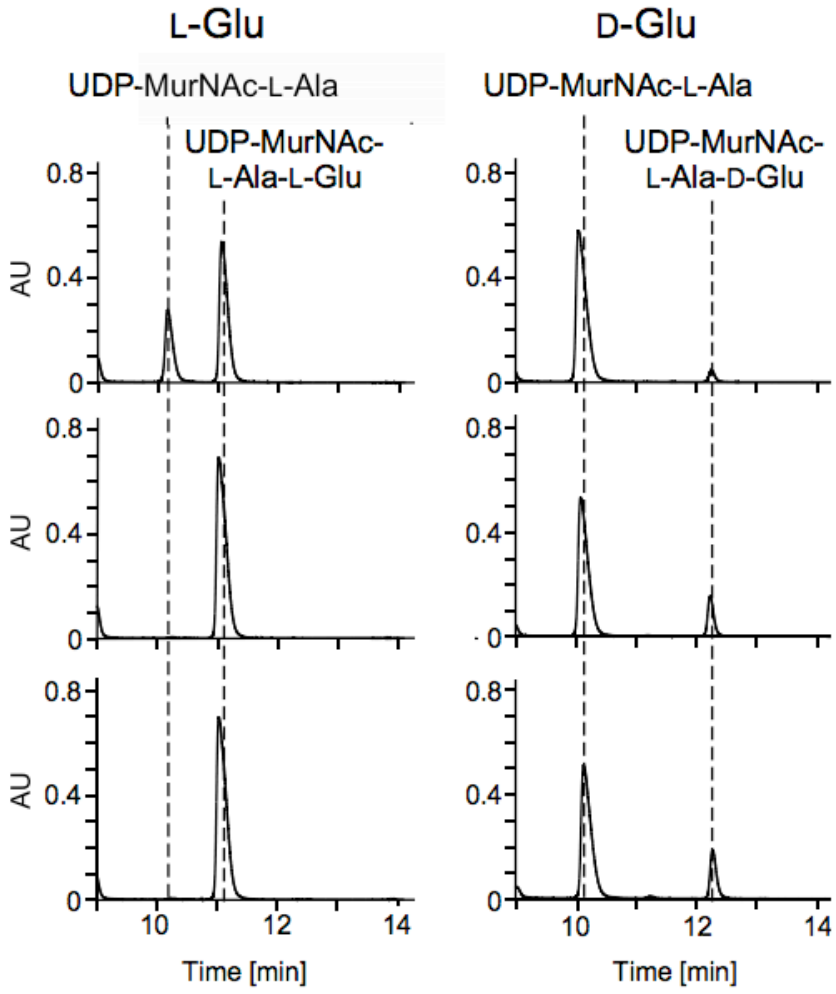

Figure 3.4 UDP-MurNAc-L-Ala-Glu synthetase activities of recombinant MurD2 and its mutants with UDP-MurNAc-L-Ala and L-Glu (left column) or D-Glu (right column) as the substrates.
HPLC traces (260 nm) of the reaction products formed with wild type, P433A, and F435L enzymes (from bottom to top) are shown.

Different from P433A- and F435L-mutated enzymes, R358K- and E197D-mutated enzymes changed the substrate specificity. As shown in Figure 3.5, The R358K-mutated enzyme lost L-Glu ligase activity but maintained slight activity against D-Glu. The E197D-mutated enzyme showed almost the same activity levels with L-Glu and D-Glu. I then constructed an E197D/R358K double-mutated enzyme. The enzyme accepted only D-Glu, suggesting that only these two amino acid residues in MurD2 control the acceptability of substrates with different stereochemistries

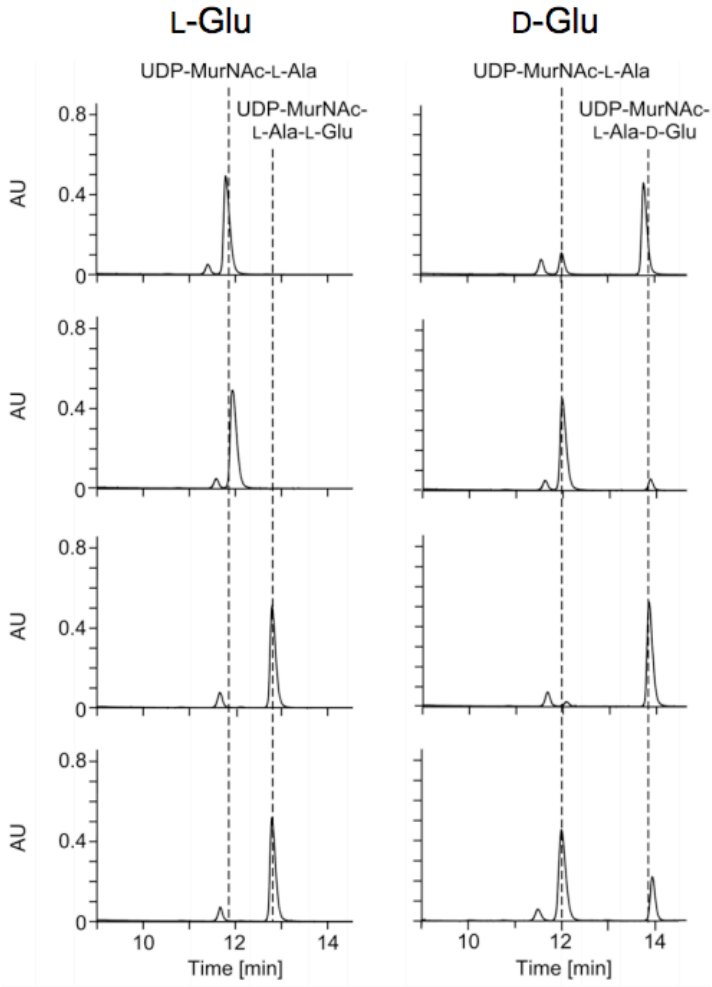

Figure 3.5 UDP-MurNAc-L-Ala-Glu synthetase activities of recombinant MurD2 and its mutants with UDP-MurNAc-L-Ala and L-Glu (left column) or D-Glu (right column) as the substrates.
HPLC traces (260 nm) of the reaction products formed with wild type, E197D, R358K, and E197D/R358K enzymes (from bottom to top) are shown.

3.3.2.3 Proposed isomer recognition mechanism of MurD2

Docking studies of a UDP-MurNAc-L-Ala-phosphate and an amino acid substrate (L-Glu or D-Glu) in the MurD2 model of the substrate-binding state predicted that the amino group of L-Glu faced toward the phosphocarboxyl carbon of the UDP-MurNAc-L-Ala-phosphate molecule, while that of D-Glu protruded toward the phosphate moiety of the UDP-MurNAc-L-Ala-phosphate molecule.

The estimated distance between the phosphocaroxyl carbon and the amino group of L-Glu was 3.0 Å in the docking model. However, the distance between the phosphocarboxyl carbon and the amino group of D-Glu was 3.7 Å. It showed that MurD2 could not orient D-Glu toward the intermediate to ligate it owing to the alteration in the shape of the Glu recognition site caused by the protruding side chains of Glu197 and Arg358 (Figure 3.6).

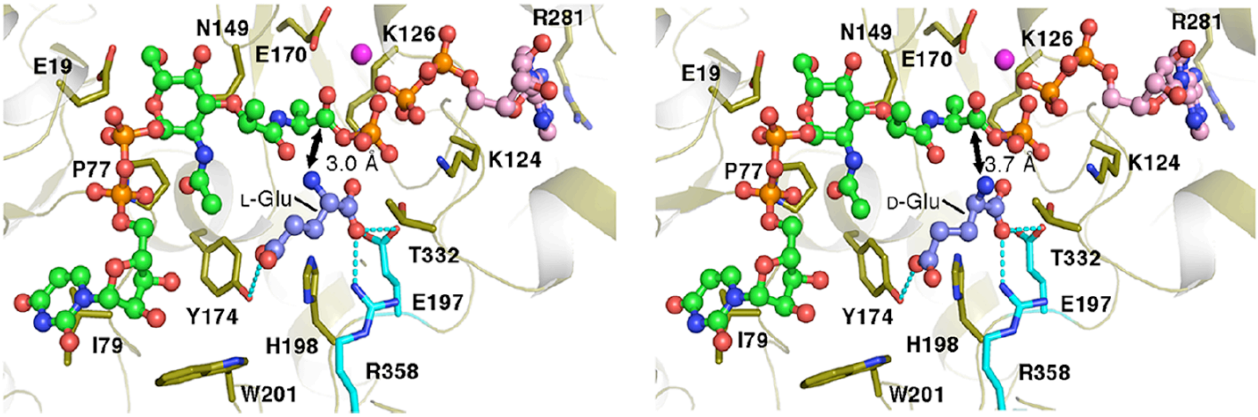

Figure 3.6 Close-up views of the active site cavity of the MurD2 quinary complex models with UDP-MurNAc-L-Ala-phosphate, ADP, Mg^{2+}, and L-Glu (left) or D-Glu (right).
The UDP-MurNAc-L-Ala-phosphate and ADP molecules are indicated with green and pink ball stick models, respectively. The Mg^{2+} irons are indicated with magenta sphere models. The L-Glu and D-Glu molecules, as the substrates, are indicated with blue ball stick models. Glu197 and Arg358 are indicated with cyan stick models.

3.3.3 Changing the $MurD_{ec}$ substrate specificity

I next tried to change the substrate specificity of $MurD_{ec}$ using the same strategy. Four amino acid residues, Asp182, Lys348, Ala414, and Leu416 of $MurD_{ec}$ were replaced with the corresponding residues of MurD2. Since both of the residues R358 and E197 in MurD2 were important for L-Glu recognition, I also constructed the D182E/K348R double-mutated enzyme. All the mutants were used for in vitro experiment.

3.3.3.1 Preparation of recombinant enzymes of $MurD_{ec}$ mutants

His-tagged recombinant enzymes of $MurD_{ec}$ mutants were successfully expressed in a soluble form. The obtained recombinant enzymes of were subjected to SDS-PAGE analysis to confirm the molecular size and purity (Figure 3.7)

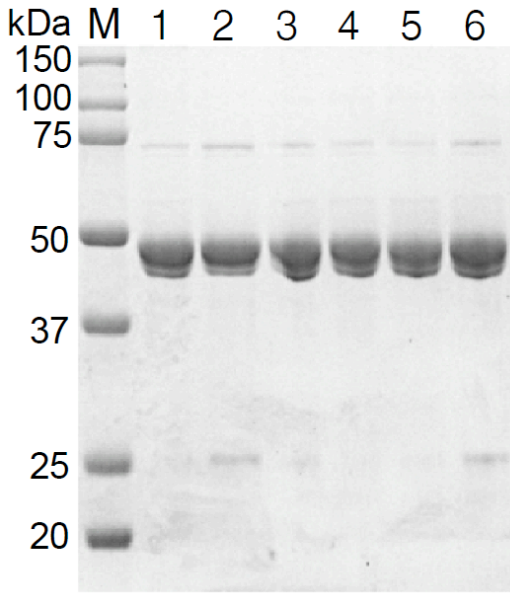

Figure 3.7 SDS-PAGE analysis of purified recombinant $MurD_{ec}$ and its mutants (48.2 kDa).
M, marker; 1, wild type; 2, D182E; 3, K348R; 4, A414P; 5, L416F; 6, D182E/K348R

3.3.3.2 In vitro experiments with $MurD_{ec}$ mutants

To check whether the substrate specificity was changed, the $MurD_{ec}$ mutants were used for in vitro experiment using L-Glu or D-Glu as substrate.

However, all four $MurD_{ec}$ single-mutanted enzymes showed the same activity as the wild-type enzyme. Moreover, the D182E/K348R double-mutated enzyme also accepted only D-Glu (Figure 3.8). The results were in good agreement with a previous report that $MurD_{ec}$ had a very strict substrate specificity (9).

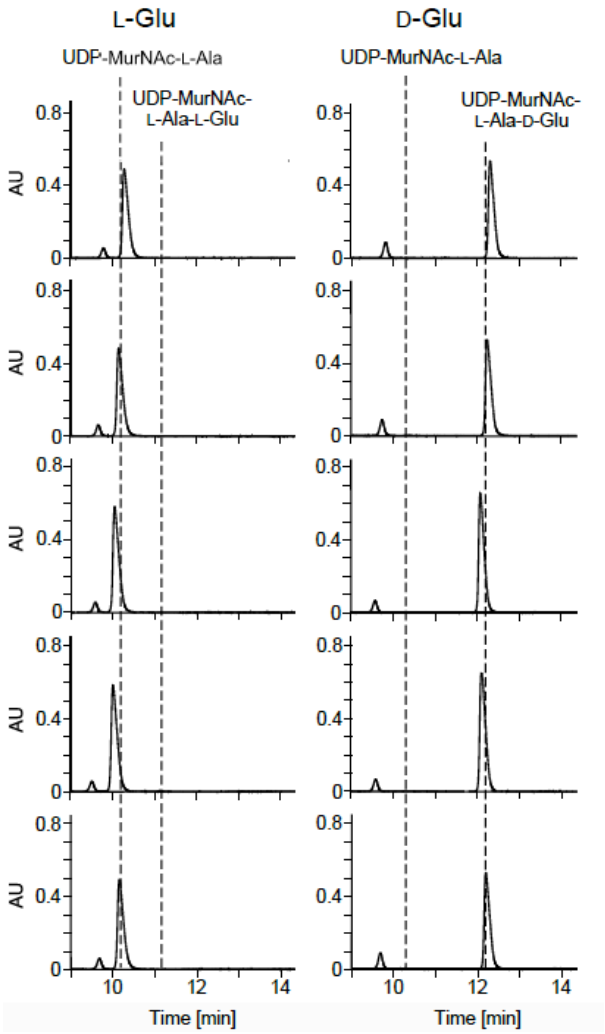

Figure 3.8 UDP-MurNAc-L-Ala-Glu synthetase activities of recombinant $MurD_{ec}$ and its mutants with UDP-MurNAc-L-Ala and L-Glu (left column) or D-Glu (right column) as the substrates.
HPLC traces (260 nm) of the reaction products formed with wild type, D182E, K348R, A414P, and L416F enzymes (from bottom to top) are shown.

3.3.4 Changing the $MurD_{sm}$ substrate specificity

Since it was difficult to change the substrate specificity of $MurD_{ec}$, I tried to perform the same experiments using another MurD enzyme. I selected MurD of *Streptococcus mutans* ($MurD_{sm}$). This $MurD_{sm}$ possesses a 28% identity with MurD2 of *X. oryzae*. Also, by sequence alignment, I found that R358 in MurD2, which is the key residue for L-Glu recognition, was also conserved at position 358 in $MurD_{sm}$ (Figure 3.9). So, I proposed that $MurD_{sm}$ might have a L-Glu ligase activity.

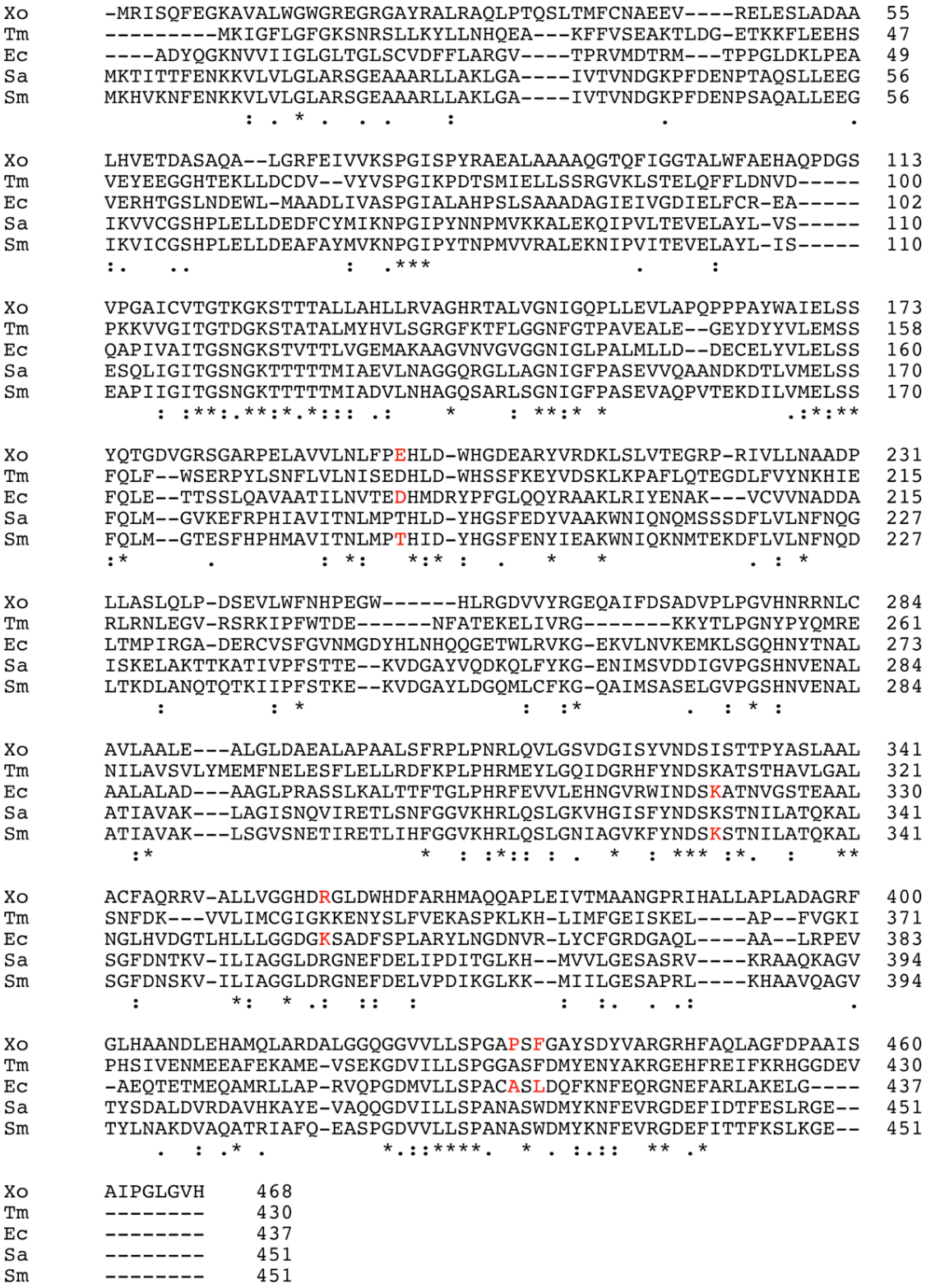

Figure 3.9 Sequence alignment of MurD2 and MurDs.

The alignment was constructed using Clustal Omega (https://www.ebi.ac.uk/Tools/msa/clustalo/). Xo, MurD2 of *X. oryzae*; Tm, MurD of *Thermotoga maritime*; Ec, MurD of *E. coli*; Sa, MurD of *Streptococcus agalactiae*; Sm, MurD of *S. mutans*. The residues mutated in this chapter are marked in red.

3.3.4.1 Substrate specificity of $MurD_{sm}$

3.3.4.1.1 Preparation of recombinant enzyme of $MurD_{sm}$

His-tagged recombinant enzyme of $MurD_{sm}$ was successfully expressed in a soluble form. The obtained recombinant enzyme was subjected to SDS-PAGE analysis to confirm the molecular size and purity (Figure 3.10).

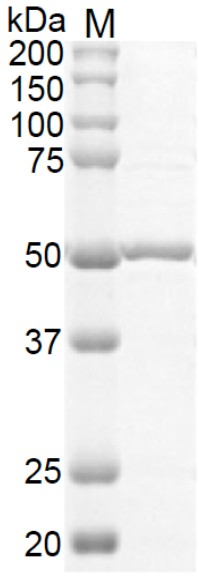

Figure 3.10 SDS-PAGE analysis of purified recombinant $MurD_{sm}$ (51.1 kDa).
M, marker

3.3.4.1.2 In vitro experiments with $MurD_{sm}$ wild type

To confirm the substrate specificity of $MurD_{sm}$, the recombinant enzyme was used for in vitro experiment using L-Glu or D-Glu as the substrate. As shown in Figure 3.11, $MurD_{sm}$ could accept D-Glu, just like $MurD_{ec}$. Moreover, L-Glu was also slightly accepted by $MurD_{sm}$ in contrast to $MurD_{ec}$.

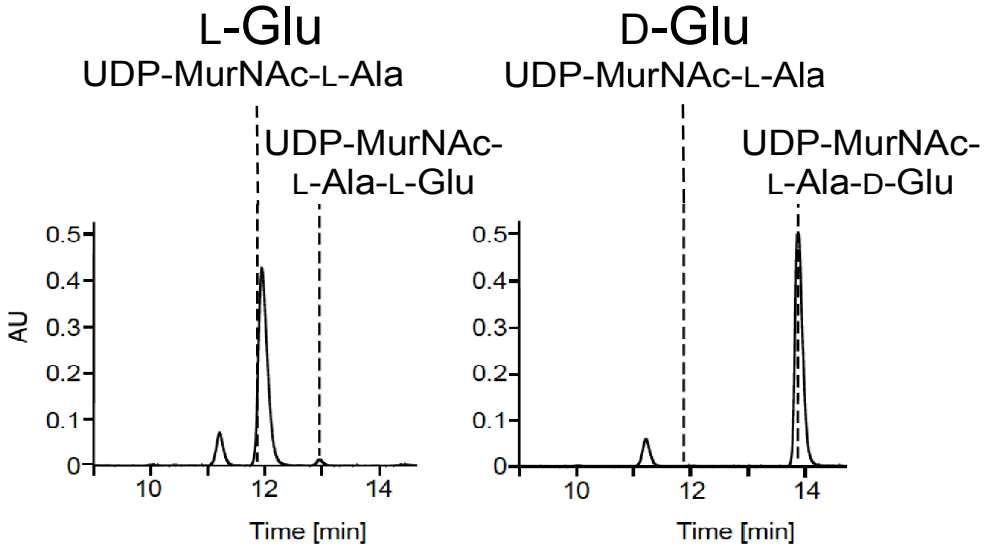

Figure 3.11 UDP-MurNAc-L-Ala-Glu synthetase activities of recombinant $MurD_{sm}$ with UDP-MurNAc-L-Ala and L-Glu (left column) or D-Glu (right column) as the substrates.
HPLC traces (260 nm) of the reaction products are shown.

3.3.4.2 Site-direct mutagenesis of $MurD_{sm}$

Since $MurD_{sm}$ could slightly accept L-Glu, I used $MurD_{sm}$ for substrate specificity changing experiments.

As mentioned before, R358, which is important for L-Glu recognition in MurD2, is also conserved in $MurD_{sm}$. By sequence alignment (Figure 3.9), I found that E197 in MurD2, which is another key residue for L-Glu recognition, appeared to correspond to T192 in $MurD_{sm}$. So, I constructed a $MurD_{sm}$ mutant to replace the Thr residue at 192 with Glu and checked whether the substrate specificity was changed.

3.3.4.2.1 Preparation of recombinant enzyme of $MurD_{sm}$_T192E

His-tagged recombinant enzyme of $MurD_{sm}$_T192E was successfully expressed in a soluble form. The obtained recombinant enzyme was subjected to SDS-PAGE analysis to confirm the molecular size and purity (Figure 3.12).

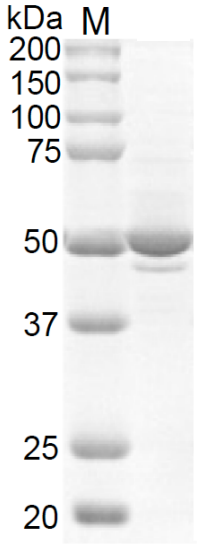

Figure 3.12 SDS-PAGE analysis of recombinant $MurD_{sm}$_T192E (51.1 kDa).
M, marker

3.3.4.2.2 In vitro experiment with $MurD_{sm}$_T192E mutant

To confirm the substrate specificity of $MurD_{sm}$_T192E mutant, the recombinant enzyme was used for in vitro experiment using L-Glu or D-Glu as substrate. However, the mutated enzyme accepted only D-Glu (Figure 3.13).

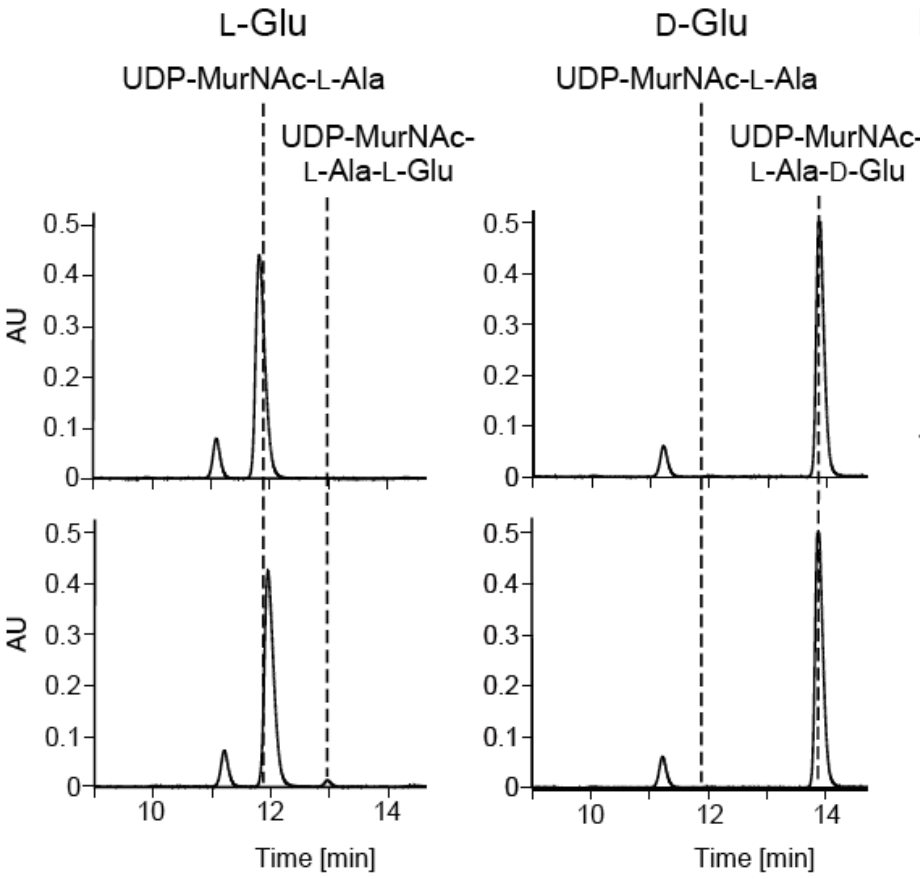

Figure 3.13 UDP-MurNAc-L-Ala-Glu synthetase activities of recombinant $MurD_{sm}$ and its mutant with UDP-MurNAc-L-Ala and L-Glu (left column) or D-Glu (right column) as the substrates.
HPLC traces (260 nm) of the reaction products formed with T192E mutant (top) and wild type (bottom) are shown.

3.3.4.3 Random mutagenesis of $MurD_{sm}$

3.3.4.3.1 Searching for $MurD_{sm}$ mutants which could accept L-Glu

Next, I tried to isolate a mutated $MurD_{sm}$ that could accept L-Glu using random mutagenesis. Briefly, the *murD2* and *murL* genes were obtained by shotgun cloning experiments using D-Glu auxotrophic *E. coli* mutant (WM335) as the host. The strain lacks Glu isomerase (MurI) and can grow by complementation with *murI*, *murD2/murL*, or D-Glu supplementation but not with $murD_{sm}$/*murL*. However, when the substrate specificity of $MurD_{sm}$ was changed from D-Glu to L-Glu, $murD_{sm}$/*murL* genes could complement the strain WM335. Therefore, I constructed a plasmid library containing mutated $murD_{sm}$ using error-prone PCR and introduced the library into strain WM335 together with the *murL* gene. Colony selection was performed on a plate without D-Glu.

As a result, I obtained 28 colonies on LB plate. The sequences of the colonies were determined and all the inserted DNAs in plasmids were confirmed to possess K330T mutations.

3.3.4.3.2 Preparation of recombinant enzyme of $MurD_{sm}$_K330T

To confirm the substrate specificity of $MurD_{sm}$_K330T, I prepared the recombinant enzyme for in vitro experiment. His-tagged recombinant enzyme of $MurD_{sm}$_K330T was successfully expressed in a soluble form. The obtained recombinant enzyme was subjected to SDS-PAGE analysis to confirm the molecular size and purity (Figure 3.14).

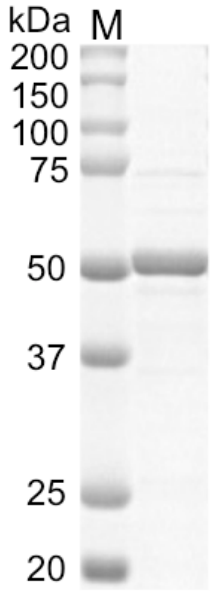

Figure 3.14 SDS-PAGE analysis of recombinant $MurD_{sm}$_K330T (51.1 kDa).
M, marker

3.3.4.3.3 In vitro assay with $MurD_{sm}$_K330T mutant

To confirm the substrate specificity of $MurD_{sm}$_K330T mutant, the recombinant enzyme was used for in vitro experiment using L-Glu or D-Glu. As shown in Figure 3.15, the enzyme still showed high activity with D-Glu. However, the mutant showed the higher activity with L-Glu than that of the parental enzyme (3.7-fold), suggesting K330 was important for $MurD_{sm}$ substrate recognition.

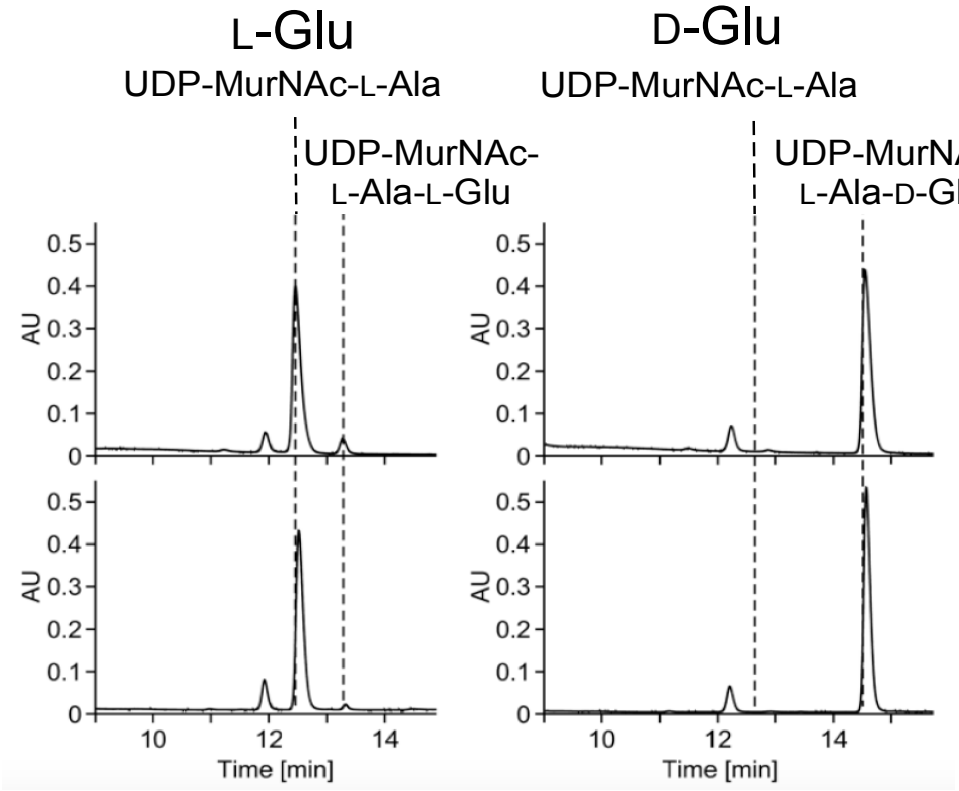

Figure 3.15 UDP-MurNAc-L-Ala-Glu synthetase activities of recombinant $MurD_{sm}$ and $MurD_{sm}$_K330T mutant with UDP-MurNAc-L-Ala and L-Glu (left column) or D-Glu (right column) as the substrates.
HPLC traces (260 nm) of the reaction products formed with K330T mutant (top) and wild type (bottom) are shown.

3.3.4.3.4 In vitro assay with $MurD_{ec}$_K319T mutant

By aligning the amino acid sequences of $MurD_{ec}$ and $MurD_{sm}$, I found that K330 in $MurD_{sm}$, which is the key residue for substrate recognition, appeared to correspond to K319 in $MurD_{ec}$. To confirm the function of K319 in $MurD_{ec}$, I constructed a K319T-mutated $MurD_{ec}$ for in vitro experiment. As shown in Figure 3.16, this mutant slightly accepted L-Glu, in contrast to the parental enzyme, which accepted no L-Glu, showing K319 was important for $MurD_{ec}$ substrate recognition.

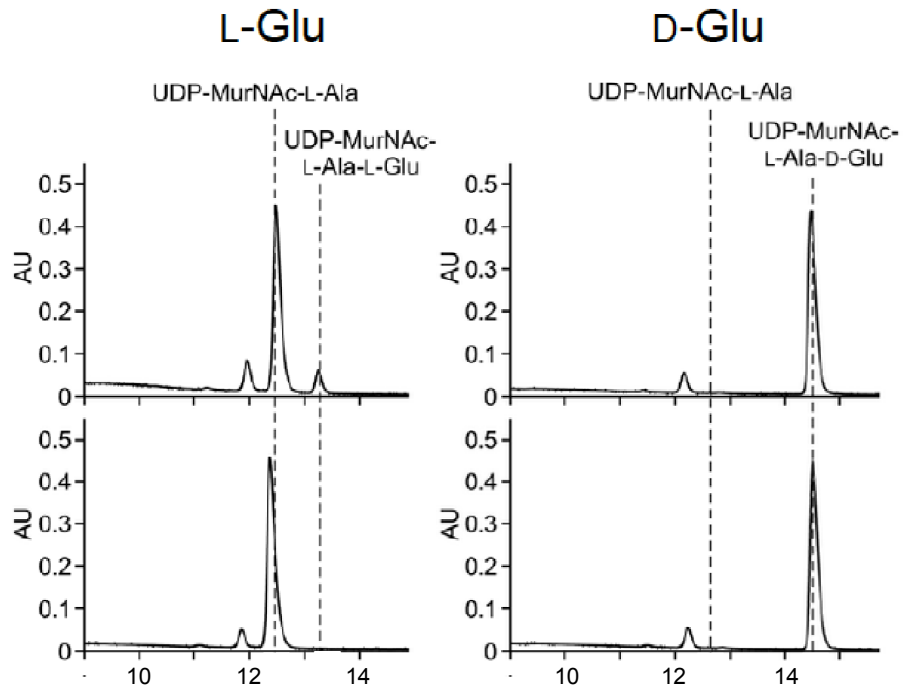

Figure 3.16 UDP-MurNAc-L-Ala-Glu synthetase activities of recombinant $MurD_{ec}$ and $MurD_{sm}$_K319T mutant with UDP-MurNAc-L-Ala and L-Glu (left column) or D-Glu (right column) as the substrates.
HPLC traces (260 nm) of the reaction products formed with K319T mutant (top) and wild type (bottom) are shown.

3.4 Discussion

In this chapter, I completely converted the chiral specificity of MurD2 from L-Glu to D-Glu by incorporating two amino acid substitutions. However, to identify the detailed substrate recognition mechanism of MurD2, crystal structure analysis of the enzyme is necessary in the future work.

Also, I changed the chiral specificity of MurD to accept L-Glu by incorporating one amino acid substitution. However, all the mutated MurD enzymes possessed the same mutations and showed low activity with L-Glu. To obtain an additional mutation in MurD, I changed the screening conditions to select a mutant that had a more rapid growth rate than that of strain WM335 carrying *murD*$_{sm}$*_K330T*/*murL*. However, the selected colonies had no additional mutations in the *murD*$_{sm}$*_K330T* gene.

I next combined the K319T mutation with the D182E/K348R mutations. I constructed the following *murD*$_{ec}$ mutated genes: D182E/K319T, K319T/K348R, D182E/K319T/K348R, K319I, D182E/K319I, K319I/K348R, and D182E/K319I/K348R mutant genes, which were used for complementation assay with coexpression of *murL* in WM335. However, only the K319T gene could complement the mutant.

Chapter 4

Conclusion

D-Glutamate (Glu) supplied by Glu racemases or D-amino acid transaminase is utilized for peptidoglycan biosynthesis in microorganisms. Comparative genomics has shown that some microorganisms, including *Xanthomonas oryzae*, perhaps have no orthologues of these genes.

To identify the D-Glu biosynthesis pathway, I performed shotgun cloning experiments with a D-Glu auxotrophic *Escherichia coli* mutant as the host and *X. oryzae* as the DNA donor. I obtained complementary genes, XOO_1319 and XOO_1320, which are annotated as a hypothetical protein and MurD (UDP-MurNAc-L-Ala-D-Glu synthetase), respectively. By detailed *in vitro* analysis, I revealed that XOO_1320 (MurD2) is an enzyme to ligate L-Glu to UDP-MurNAc-L-Ala for the first example of MurD utilizing L-Glu, and that XOO_1319 (MurL) is a novel enzyme catalyzing epimerization of the terminal L-Glu of the product in the presence of ATP and Mg^{2+}.

MurD2 possess 26% identity with canonical *E.coli* MurD, which ligates D-Glu to UDP-MurNAc-L-Ala. To understand how MurD2 recognize the isomer substrate, a MurD2 structure was estimated based on *E. coli* MurD structure by docking simulations. By replacing two amino acid residues in MurD2 with the corresponding amino acid residues in MurD, I obtained a mutant MurD2 that accepted only D-Glu. Also, by a random mutagenesis with MurD from *Streptococcus mutans,* I found an important amino acid residue for MurD isomer recognition and mutated MurD that had one amino acid substitution could slightly accept L-Glu. Thus, I revealed that only a few amino acid residues in MurD/MurD2 control the acceptability of substrates with different stereochemistries.

Reference

1. Hiratsuka, T., Furihata, K., Ishikawa, J., Yamashita, H., Itoh, N., Seto, H., Dairi, T. (2008). An alternative menaquinone biosynthetic pathway operating in microorganisms. *Science*, **321**, 1670–1673.
2. Satoh, Y., Kuratsu, M., Kobayashi, D., Dairi, T. (2014). New gene responsible for para-aminobenzoate biosynthesis. *Journal of bioscience and bioengineering*, **117**, 178–183.
3. Van Heijenoort, J. (2001). Recent advances in the formation of the bacterial peptidoglycan monomer unit. *Natural product reports*, **18**, 503–519.
4. El Zoeiby, A., Sanschagrin, F., Levesque, R. C. (2003). Structure and function of the Mur enzymes: development of novel inhibitors. *Molecular microbiology*, **47**, 1–12.
5. Moraes, G. L., Gomes, G. C., De Sousa, P. R. M., Alves, C. N., Govender, T., Kruger, H. G., Maguire, G. E. M, Lamichhane, G., Lameira, J. (2015). Structural and functional features of enzymes of *Mycobacterium tuberculosis* peptidoglycan biosynthesis as targets for drug development. *Tuberculosis*, **95**, 95–111.
6. Gautam, A., Vyas, R., & Tewari, R. (2011). Peptidoglycan biosynthesis machinery: a rich source of drug targets. *Critical reviews in biotechnology*, **31**, 295–336.
7. Doublet, P., Van Heijenoort, J., Bohin, J. P., Mengin-Lecreulx, D. (1993). The *murI* gene of *Escherichia coli* is an essential gene that encodes a glutamate racemase activity. *Journal of Bacteriology*, **175**, 2970–2979.
8. Thorne, C. B., Gómez, C. G., Housewright, R. D. (1955). Transamination of D-amino acids by *Bacillus subtilis*. *Journal of bacteriology*, **69**, 357–362.
9. Pratviel-Sosa, F., Acher, F., Trigalo, F., Blanot, D., Azerad, R., van Heijenoort, J. (1994). Effect of various analogues of D-glutamic acid on the D-glutamate-adding enzyme from *Escherichis coli*. *FEMS microbiology letters*, **115**, 223–228.
10. Ogasawara, Y., Dairi, T. (2018). Peptide epimerization machineries found in microorganisms. *Frontiers in microbiology*, **9**, 156.
11. Schmidt, D. M., Hubbard, B. K., Gerlt, J. A. (2001). Evolution of enzymatic activities in the enolase superfamily: functional assignment of unknown proteins in *Bacillus subtilis* and *Escherichia coli* as L-Ala-D/L-Glu epimerases. *Biochemistry*, **40**, 15707–15715.

12. Gulick, A. M., Schmidt, D. M., Gerlt, J. A., Rayment, I. (2001). Evolution of enzymatic activities in the enolase superfamily: crystal structures of the L-Ala-D/L-Glu epimerases from *Escherichia coli* and *Bacillus subtilis*. *Biochemistry*, **40**, 15716–15724.
13. Stachelhaus, T., Walsh, C. T. (2000). Mutational analysis of the epimerization domain in the initiation module PheATE of gramicidin S synthetase. *Biochemistry*, **39**, 5775–5787.
14. Luo, L., Kohli, R. M., Onishi, M., Linne, U., Marahiel, M. A., Walsh, C. T. (2002). Timing of epimerization and condensation reactions in nonribosomal peptide assembly lines: kinetic analysis of phenylalanine activating elongation modules of tyrocidine synthetase B. *Biochemistry*, **41**, 9184–9196.
15. Morinaka, B. I., Vagstad, A. L., Helf, M. J., Gugger, M., Kegler, C., Freeman, M. F., Piel, J. (2014). Radical S-Adenosyl Methionine Epimerases: Regioselective introduction of diverse D-Amino acid patterns into peptide natural products. *Angewandte Chemie International Edition*, **53**, 8503–8507.
16. Xie, L., Miller, L. M., Chatterjee, C., Averin, O., Kelleher, N. L., Van Der Donk, W. A. (2004). Lacticin 481: in vitro reconstitution of lantibiotic synthetase activity. *Science*, **303**, 679–681.
17. Tang, W., Jiménez-Osés, G., Houk, K. N., Van Der Donk, W. A. (2015). Substrate control in stereoselective lanthionine biosynthesis. *Nature chemistry*, **7**, 57–64.
18. Yang, X., Van der Donk, W. A. (2015). Post-translational introduction of D-alanine into ribosomally synthesized peptides by the dehydroalanine reductase NpnJ. *Journal of the American Chemical Society*, **137**, 12426–12429.
19. Sharma, P., Bora, L. C., Puzari, K. C. (2017). Review on bacterial blight of rice caused by *Xanthomonas oryzae pv. oryzae:* different management approaches and role of Pseudomonas fluorescens as a potential biocontrol agent. *International Journal of Current Microbiology and Applied Sciences*, **6**, 982–1005.
20. Ochiai, H., Inoue, Y., Takeya, M., Sasaki, A., Kaku, H. (2005). Genome sequence of *Xanthomonas oryzae* pv. *oryzae* suggests contribution of large numbers of effector genes and insertion sequences to its race diversity. *Japan Agricultural Research Quarterly: JARQ*, **39**, 275–287.

21. Dougherty, T. J., Thanassi, J. A., Pucci, M. J. (1993). The *Escherichia coli* mutant requiring D-glutamic acid is the result of mutations in two distinct genetic loci. *Journal of bacteriology*, **175**, 111–116.
22. Purcell, A. H. (1997). *Xylella fastidiosa*, a regional problem or global threat?. *Journal of Plant Pathology*, **79**, 99–105.
23. Denton, M., Kerr, K. G. (1998). Microbiological and clinical aspects of infection associated with *Stenotrophomonas maltophilia*. *Clinical microbiology reviews*, **11**, 57–80.
24. Hayashi, S., Satoh, Y., Ujihara, T., Takata, Y., Dairi, T. (2016). Enhanced production of polyunsaturated fatty acids by enzyme engineering of tandem acyl carrier proteins. *Scientific reports*, **6**, 35441.
25. Marfey, P. (1984). Determination of D-amino acids. II. Use of a bifunctional reagent, 1,5-difluoro-2,4-dinitrobenzene. *Carlsberg Research Communications*, **49**, 591.
26. Raymond, J. B., Price, N. P., Pavelka Jr, M. S. (2003). A method for the enzymatic synthesis and HPLC purification of the peptidoglycan precursor UDP-*N*-acetylmuramic acid. *FEMS microbiology letters*, **229**, 83–89.
27. Fujii, K., Ikai, Y., Oka, H., Suzuki, M., Harada, K. I. (1997). A nonempirical method using LC/MS for determination of the absolute configuration of constituent amino acids in a peptide: combination of Marfey's method with mass spectrometry and its practical application. *Analytical Chemistry*, **69**, 5146–5151.
28. Bertrand, J. A., Auger, G., Fanchon, E., Martin, L., Blanot, D., van Heijenoort, J., Dideberg, O. (1997). Crystal structure of UDP-*N*-acetylmuramoyl-L-alanine: D-glutamate ligase from *Escherichia coli*. *The EMBO journal*, **16**, 3416–3425.
29. Bertrand, J. A., Auger, G., Martin, L., Fanchon, E., Blanot, D., Le Beller, D., van Heijenoort, J., Dideberg, O. (1999). Determination of the MurD mechanism through crystallographic analysis of enzyme complexes. *Journal of molecular biology,* **289**, 579−590.
30. Saio, T., Ogura, K., Kumeta, H., Kobashigawa, Y., Shimizu, K., Yokochi, M., Kodama, K., Yamaguchi, H., Tsujishita, H., Inagaki, F. (2015). Ligand-driven

conformational changes of MurD visualized by paramagnetic NMR. *Scientific reports*, **5**, 16685.

31. Perdih, A., Solmajer, T. (2012). MurD ligase from *Escherichia coli*: *C*-terminal domain closing motion. *Computational and Theoretical Chemistry*, **979**, 73–81.
32. Šink, R., Barreteau, H., Patin, D., Mengin-Lecreulx, D., Gobec, S., Blanot, D. (2013). MurD enzymes: some recent developments. *Biomolecular concepts*, **4**, 539–556.
33. Šink, R., Kotnik, M., Zega, A., Barreteau, H., Gobec, S., Blanot, D., Dessen, A., Contreras-Martel, C. (2016). Crystallographic study of peptidoglycan biosynthesis enzyme MurD: domain movement revisited. *PLoS One*, **11**, e0152075

Acknowledgements

At beginning, I would like to express my sincerest thanks and gratitude to my supervisor, Professor Tohru Dairi, for his guidance and support of five years during both my master's and doctoral studies. His invaluable guidance and kind suggestions have given me enormous help towards my research. Besides, I have learnt from him not only the technical knowledge but also the attitude as a researcher.

Secondly, I would like to express my great thanks to assistant professors Yasuharu Satoh and Yasushi Ogasawara for their advice and encouragements on my research. Appreciations are also extended to all my lab mates for their support and the enjoyable days with them.

I am grateful to Professor Tohru Yoshimura at Nagoya University for kindly providing *E. coli* WM335. I also thank Dr. Eri Fukushi at Hokkaido University for measuring NMR spectra. Great thanks also go to Professor Hiroyuki Morita at Toyama University for his kindness and cooperation on this research.

Finally, I am extremely grateful to my family for the endless encouragement and unconditional love.